Power Systems Design
EUROPE

Empowering Global Innovation — July/August 2010

Charge pump minimizes EMI while boosting the supply for ISO compliant high-speed CAN Tx/Rx

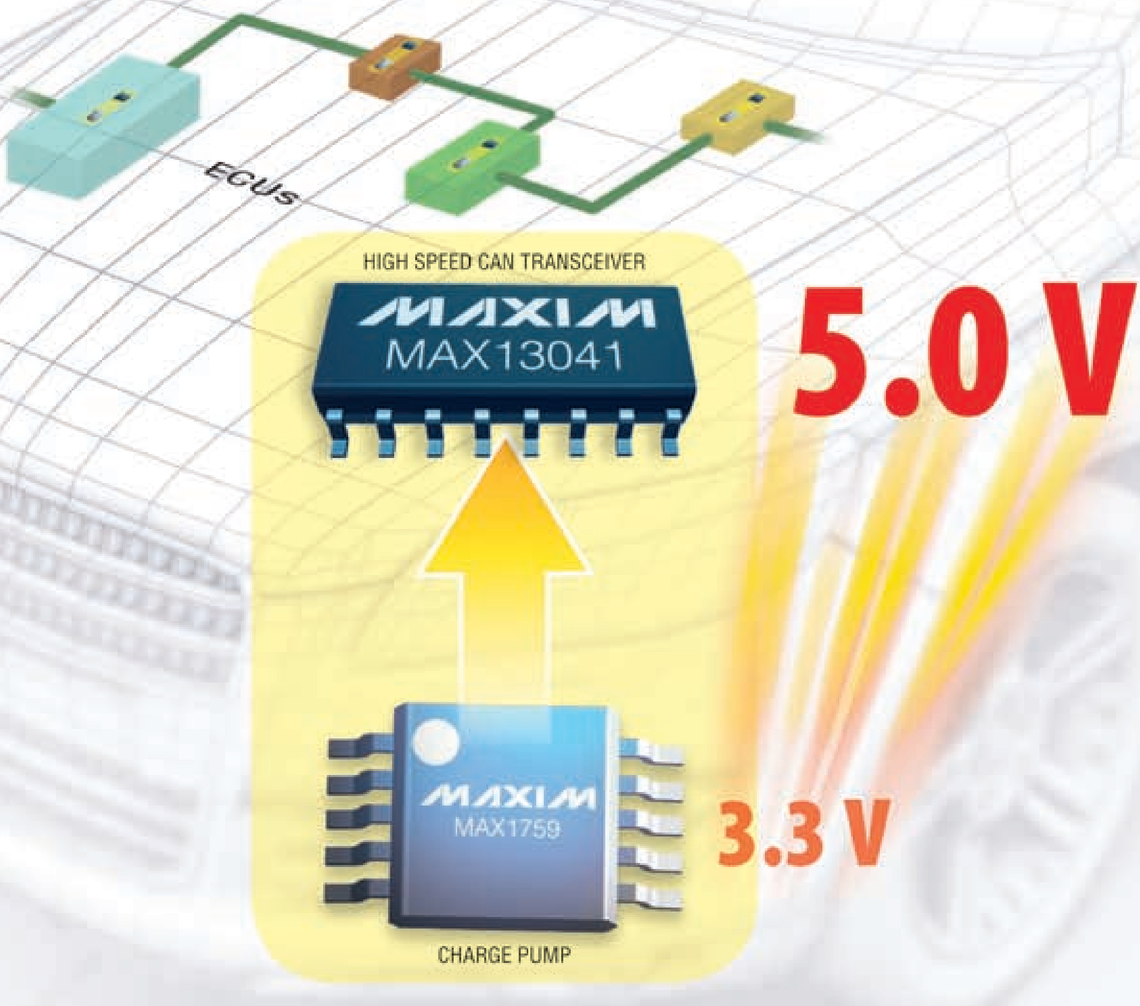

PSDE Green Power
ENERGY EFFICIENCY

Special Report – Automotive Electronics

ISSN: 1613-6365

Power Systems Design EUROPE

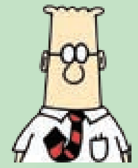

Dilbert – 56

ViewPoint
Servicing Automotive, By Cliff Keys, Editor-in-Chief, PSDE 4

Industry News: Web Exclusive Content (www.powersystemsdesign.com)

PSDE PowerLine
Auto Load Dump & Cold-Crank Solution 6

PSDE PowerPlayer
Delivering Automotive Solutions, By Dave Bell, Intersil Corporation 8

MarketWatch
Electric Vehicles Need More Power! By Jon Cropley, IMS Research 10

Design Tips
Power Supply Development Diary – Part V, By Dr. Ray Ridley, Ridley Engineering 11

TechTalk
Driving on Solar Panels, Reported By Cliff Keys, Editor-in-Chief, PSDE 14

Cover Story
Powering CAN, By Robert Regensburger, Maxim Integrated Products 16

Digital Isolation
Digital Isolators, By Don Alfano, Silicon Laboratiories 22

Special Report – Automotive Electronics
Integrated Driving, By Patrick Sullivan, Avago Technologies 26
Current Sensing in HEVs, By Shaun Milano and Mike Doogue, Allegro MicroSystems Inc 29
Drive with Infineon's EiceDRIVERs™, By Laurent Beaurenaut, Infineon Technologies 32
Next Generation Automotive, By Benjamin Jackson, International Rectifier 34
Essential Multicell Monitoring, By Jon Munson, Linear Technology Corporation 37
Swifter, Higher, Stronger- By Dr. Thomas Wirschem, National Semiconductor 40
Autmotive Air-Con Made Easy, By Bart De Cock and Steven De Preter, ON Semiconductor 43
Shining Bright, By James Aliberti, Texas Instruments 46
Cool Running Autos, By Thomas Sleasman and Birol Sonuparlak, Rogers Corporation 50

Career Development
Rugged Vehicle Applications Drive Search for Seasoned Engineers in Heavy Equipment Industry,
By David G. Morrison, Editor, How2Power.com 53

New Products: Web Exclusive Content (www.powersystemsdesign.com)

GreenPage
Auto Gets Cleaner, Reported By Cliff Keys, Editor-in-Chief, PSDE 56

Power Systems Design Europe

AGS Media Group
146 Charles Street
Annapolis, Maryland 21401 USA
Tel: +410-295-0177
Fax: +510-217-3608
www.powersystemsdesign.com

Editorial Director, Power Systems Design China, Europe & North America
Editor-in-Chief, Power Systems Design Europe & North America
Cliff Keys
cliff.keys@powersystemsdesign.com

Contributing Editors
Liu Hong
Editor-in-Chief, Power Systems Design China
powersdc@126.com
Ash Sharma, IMS Research
ash.sharma@imsresearch.com
Dr. Ray Ridley, Ridley Engineering
RRidley@ridleyengineering.com
David Morrison, How2Power
david@how2power.com

Publishing Director
Jim Graham
jim.graham@powersystemsdesign.com

Publisher
Julia Stocks
julia.stocks@powersystemsdesign.com

Circulation Management
Kathryn Phillips
kathryn.phillips@powersystemsdesign.com

Research Director
Meghan Corneal
meghan.corneal@powersystemsdesign.com

Magazine Design
Beata Rasmus, Eyemotive
beata@eyemotive.com

Production Manager
Leo Jiang
Leow@action-new.net

Registration of copyright: January 2004
ISSN number: 1613-6365

Send address changes to: circulation@powersystemsdesign.com

Free Magazine Subscription, go to: www.powersystemsdesign.com

Volume 7, Issue 6

PSDE Green Power ENERGY EFFICIENCY

Servicing Automotive

Welcome to this special issue of Power Systems Design Europe where we take the theme of automotive technology. Within the following pages you will find an abundance of information on this increasingly popular topic as well as the in depth power related contributions, comment and articles we strive to bring to our engineering audience.

The application of electronic power devices in the automotive sphere is a true test of their survival capability under environmentally hostile conditions. It needs a specialized approach and rigourous qualification, especially in the area of power electronics. Also, with the proliferation and widening acceptance of Hybrid Electric Vehicle technology, traditional automotive technology is extended still further. This should be good news for our industry, but will inevitably take time.

The European automotive industry, particularly the prime quality German brands such as BMW, Mercedes, Porsche and Audi which use a high degree of sophisticated electronic control and gadgetry, is one of the most demanding for semiconductor firms to service. It demands a quality of electronic component far higher than found in the majority of commercial applications. The rugged environments experienced plus the extremes of temperature these devices must survive make the required skillful design engineering, manufacturing and subsequent stringent quality control a very large investment. Not a bad thing considering the many safety factors that need to be considered. These firms, I believe, well deserve the higher margins they currently command.

Following its toughest year in recent memory, the worldwide market for automotive MEMS sensors, especially pressure sensors, which are used in key applications to measure tyre pressure and engine performance, will rebound sharply in 2010, but continued high sales might lead to an overheated market that could push the industry back into depression, according to iSuppli. Global shipments are projected to reach 591.2 million units in 2010, a healthy increase of 17.8%. This growth represents a welcome turnaround after a difficult 2009 for MEMS sensors and marks the beginning of an upturn that is predicted to continue until at least the end of 2014. Europe will command over 30% share with North America accounting for the largest share in the consumption of MEMS, making up 40% of the total in 2010.

At PSD Europe, our continued quest is to give our readers the broadest and in-depth information to help bring a deeper insight to the industry. With our regular MarketWatch feature from IMS Research, David Morrison's new column on recruitment and opportunities in our industry and the in depth design feature from Dr Ray Ridley, we strive to provide a single point of reference for engineers and managers. To complement this we have the up-to-date industry and product news and information together with selected features and articles contained within our weekly web-blast, PowerSurge. If you do not receive this, please contact me and I'll get a subscription arranged.

I hope you enjoy the issue, please keep sending me your valuable feedback and enjoy our fun-strip, Dilbert at the back of the magazine.

All the best!

Cliff Keys

Editor-in-Chief, PSDE
Cliff.Keys@powersystemsdesign.com

Auto Load Dump & Cold-Crank Solution

Linear Technology announced the H-Grade version of the LT3686. The LT3686H is a 1.2A, 37VIN step-down switching regulator. The device operates within a VIN range of 3.6V to 37V with overvoltage lockout, protecting the regulator and load from transients as high as 55V, making it ideal for load dump and cold-crank conditions commonly found in automotive applications as well as 24V industrial supplies. Its internal 1.85A switch can deliver up to 1.2A of continuous output current at voltages as low as 0.8V.

Cycle-by-cycle current limit and DA current sense provide protection against fault conditions. Soft-start and frequency foldback eliminate input current surge during start-up. An optional internal regulated active load at the output via the BD pin keeps the LT3686H at full switching frequency at light loads, resulting in low, predictable output ripple above the audio and AM bands. Internal compensation and an internal boost diode reduce external component count.

The LT3686H's switching frequency is user programmable from 300kHz to 2.5MHz, enabling designers to maximize efficiency while avoiding critical noise-sensitive frequency bands such as the AM broadcast band. Its low minimum on-time enables it to provide high switching frequencies even with high step-down ratios. For example, with an input as high as 16V, it can deliver a 3.3V output using a 2MHz switching frequency. The LT3686H also uses a unique design, which ensures that it maintains constant frequency switching, even in very light load conditions. The device's 3mm x 3mm DFN-10 package and high switching frequency, which keeps the external inductor and capacitors small, provides a compact, thermally efficient footprint.

The H-grade version operates up to a junction temperature of 150˚

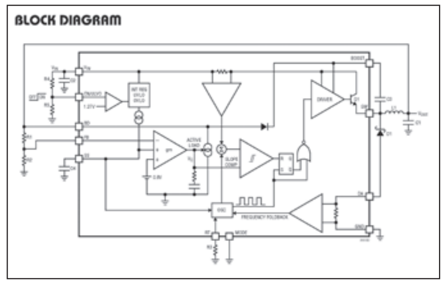

LT3686H block diagram

C, compared to the E and I grade versions' 125˚C maximum junction temperature. All electrical specifications are identical for the E, I and H grade versions. The H-grade versions are tested and guaranteed to the maximum junction temperature of 150˚C, making them especially suited to automotive and industrial applications which are subjected to high ambient temperatures.

Summary of Features: LT3686H

- Wide Input Range:
  - o Operation from 3.6V to 37V
  - o Overvoltage Lockout Protects Circuit through 55V Transients
- Low Minimum On-Time: Converts 16VIN to 3.3VOUT at 2MHz
- 1.2A Output Current
- Adjustable Frequency: 300kHz to 2.5MHz, with ±5% Accuracy
- Constant Switching Frequency at Light Loads
- Tracking & Soft Start
- Precision UVLO
- Short-Circuit Robust
- IQ in Shutdown <1uA
- Internally Compensated
- 3mm x 3mm DFN Package
- Maximum Junction Temperature of 150°C

www.linear.com/pr/3686
www.linear.com

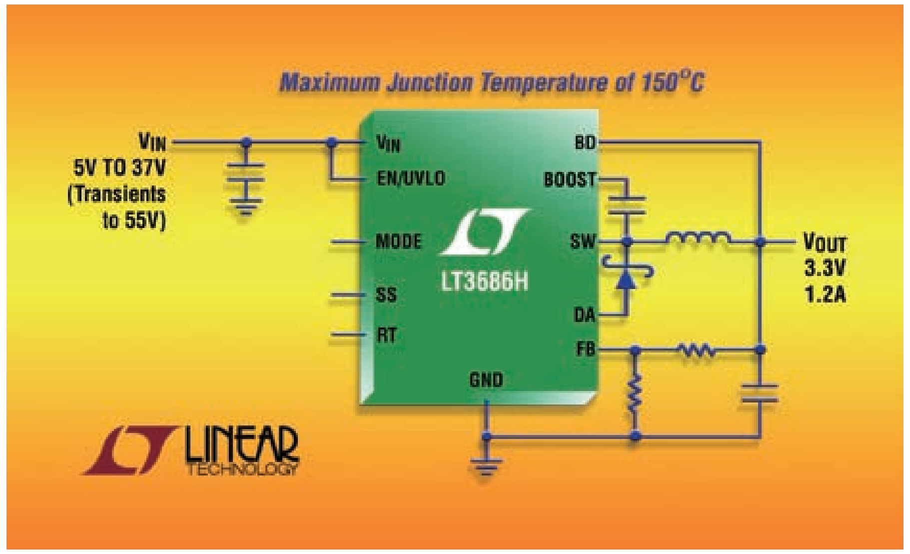

37V with 55V transient protection, 1.2A step down DC/DC converter with 150˚C maximum junction temperature

Delivering Automotive Solutions

By Dave Bell, CEO, Intersil Corporation

The automotive markets have become very creative in their application of innovative electronics technology. Every year the number of ICs per vehicle moves steadily higher. And the development of hybrid and full electric vehicles requires plenty of support and innovation from semiconductor leaders.

One of the critical items in these automotive systems is power management.

In most automotive applications, the main vehicle power supply comes directly from the 12V car battery. At engine start, the battery voltage may drop as low as 3V, a condition known as “cold crank”. Electronics connected to the car battery require protection to survive voltage transients and, in many cases, to operate normally during cold crank. Intersil’s ISL78200 represents an automotive DC-DC power supply that is fully specified to input voltages below 3V.

Systems designed to monitor the battery cells in hybrid and plug-in electric vehicles must survive plugging in or removing from a live power supply to the battery pack as well as transient voltages which may exceed 100V -- all from a supply system capable of sourcing tens of kilowatts. As the automotive industry continues its move toward better hybrids and more electric vehicles, this monitoring requirement becomes increasingly important.

There also are many types of ICs now proven in demanding industrial and high performance computing applications that can be adapted for auto systems, such as linear regulators, power supply support ICs, isolated power converters and current measurement ICs. The ISL78220 multi-phase boost controller is a good example. Based on advanced PC power technology, the ISL78220 provides a 6-phase boost function that

is well suited for stop-start systems and for supplying power in high power audio applications.

In addition to power issues, automakers also focus diligently on cost. Adapting proven consumer electronics technology used in video and audio systems to the peculiarities of the vehicle environment is a solid approach to delivering the cost-efficiencies the car makers and their tier-one suppliers demand.

For example, the auto environment needs robust video and control data transport, using devices that convert wide parallel video data to a single differential pair, then convert it back to its original parallel format. The process must be achieved cost-effectively with complete noise immunity and high EMI immunity at speeds well in excess of 1.2 Gigabits/second. The best answer -- video distribution SERDES (serialization-deserialization) technology, originally developed for commercial grade applications, and now adapted for the vehicle.

Another IC technology proven in consumer electronics and able to deliver cost-efficient, high quality video is a highly integrated LCD controller for dual-view LCD panels in front console and rear-seat automotive infotainment systems. Developed by Techwell, Inc., which Intersil acquired in 2010, these controllers already display video in main consoles and headrests for most of the major automotive suppliers. The video decoders can accept graphic content from a variety of sources such as TV tuners, DVD players, backup cameras, DTV/DMB receivers and navigation/GPS receivers.

For LCD displays used in the automotive infotainment system, Intersil’ s ISL78100 is an excellent fit as the backlight driver IC and is optimized for 3.5” to 9” LCD panels. The ISL78100 is a high-power LED backlight driver with an integrated 3A/36V FET designed to drive up to 8 high-power LEDs in series.

Advanced audio system technology is also being applied in vehicle systems, as automakers differentiate themselves with specific A/V features. They require higher power levels and higher quality audio capabilities to serve the car’s very unique and harsh operating environment. Intersil’s D2Audio group is a leader in advanced audio, with scalable Class-D power solutions and a flexible, digital feedback process that optimizes amplifier response and fits well with the power and sound requirements of the vehicle.

Intersil has broadened its portfolio of ICs designed for these innovative applications and completed the TS16949 compliance process. The company’s long and successful experience in the military and aerospace markets – with their zero-defects requirements – also is applicable to the vehicle sector. We are working hard to combine high reliability with cost-efficiency and deliver the power, video and audio that characterizes the newest, most innovative vehicles.

www.intersil.com

Electric Vehicles Need More Power!

By Jon Cropley, Director, Automotive and Transportation Group, IMS Research

It seems like every few days a different manufacturer announces plans to introduce a new electric vehicle. While this makes it difficult for analysts like me to keep up, it's all good news for power semiconductor suppliers. The value of their products in electric vehicles is much greater than in vehicles with conventional engines.

Some vehicle manufacturers already offer hybrid electric vehicles. Many others have plans to introduce them, while commercially viable plug-in hybrid and battery electric vehicles are just starting to emerge. Governments around the world are investing money to support the development efforts of the vehicle manufacturers. The Chevrolet Volt and Nissan Leaf are just two of the high profile models expected to enter volume production in the year ahead. IMS Research forecasts that demand for electric vehicles will grow steadily throughout the decade ahead from less than 600,000 in 2008 to over 12 million in 2020.

From a semiconductor supplier's point of view, growing production volumes of electric vehicles are only one side of the equation. The other side is that the value of semiconductors in an electric vehicle drivetrain is not only higher than in a conventional vehicle drivetrain: according to our research, it is over 10 times higher!

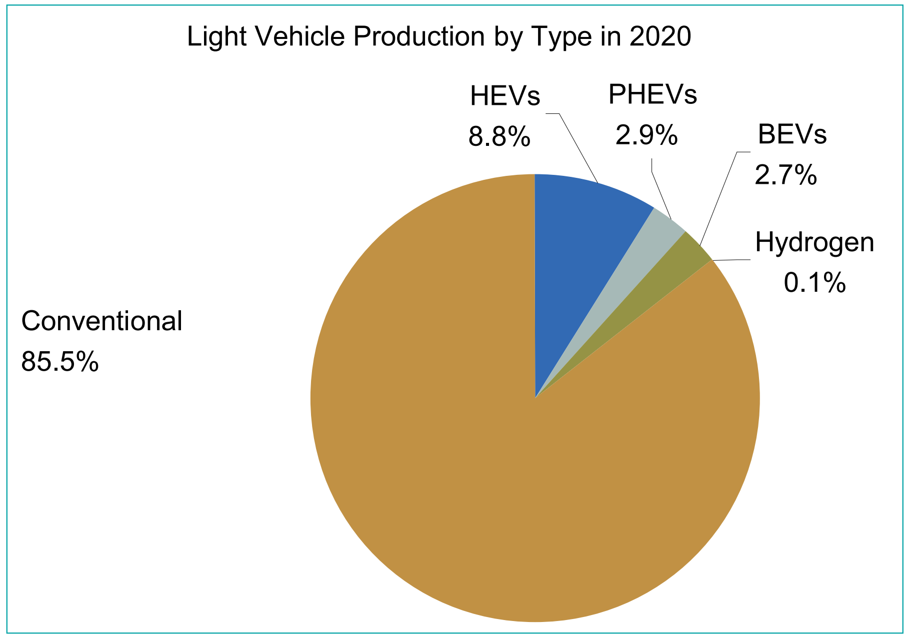

Power devices account for much of this increased semiconductor content. These vehicles have significant power IC, power discrete and power module content. Much of this is for the inverter required to drive the vehicle's main motor/generators. However, many other electric vehicle drivetrain applications require semiconductors including battery monitoring and control, DC/DC converters, AC/DC chargers and air conditioning converters.

Many semiconductor suppliers have so far found it difficult to enter the supply chain for electric vehicles. Japanese vehicle manufacturers have dominated production and have either used their own semiconductors or used semiconductors from suppliers they part own (Keiretsu partners). These barriers to market entry look set to disappear as vehicle manufacturers from other regions ramp up production and Japanese vehicle manufacturers look for competing semiconductor vendors.

As is always the case with automotive applications, semiconductors for electric vehicles must meet demanding performance requirements and must been keenly priced. However, according to IMS Research, the market could be worth over $7 billion in 2020. As world economies struggle to recover from the recent economic downturn, this developing market could provide suppliers with a rare opportunity for substantial growth.

www.imsresearch.com

Power Supply Development Diary

Part V

This article continues the series in which Dr. Ridley documents the processes involved in taking a power supply from the initial design to the full-power prototype. In part V, attention is turned to the secondary side of the converter, where snubbers and clamps are added to protect the output rectifiers.

By Dr. Ray Ridley, Ridley Engineering

Secondary Catch Diode Ringing Voltage

In Part IV of this series of articles [1], the primary voltage spikes on the switching FETs were properly controlled with improved layout and high-frequency bypass capacitors. This greatly improved the ruggedness of the converter.

Voltage spikes and ringing can also be seen on the secondary of the converter. Figure 1 shows the ringing across the catch diode with 100 VAC applied to the primary of the converter (maximum voltage rating is 280 VAC). This ringing must be suppressed before higher voltages can be applied to the converter.

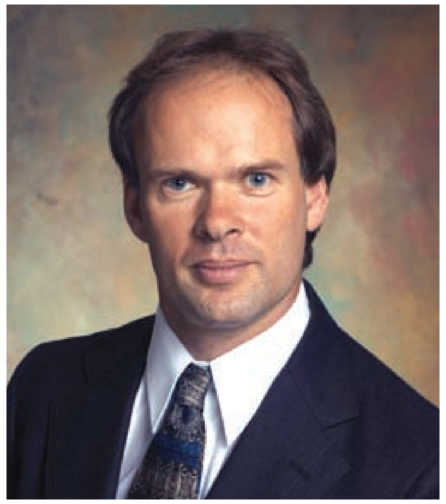

A peak voltage of 175 V is seen at the leading edge of the waveform, more than three times higher than the anticipated square wave voltage of 50 V. If this is not controlled, the secondary rectifiers will fail when full voltage is applied.

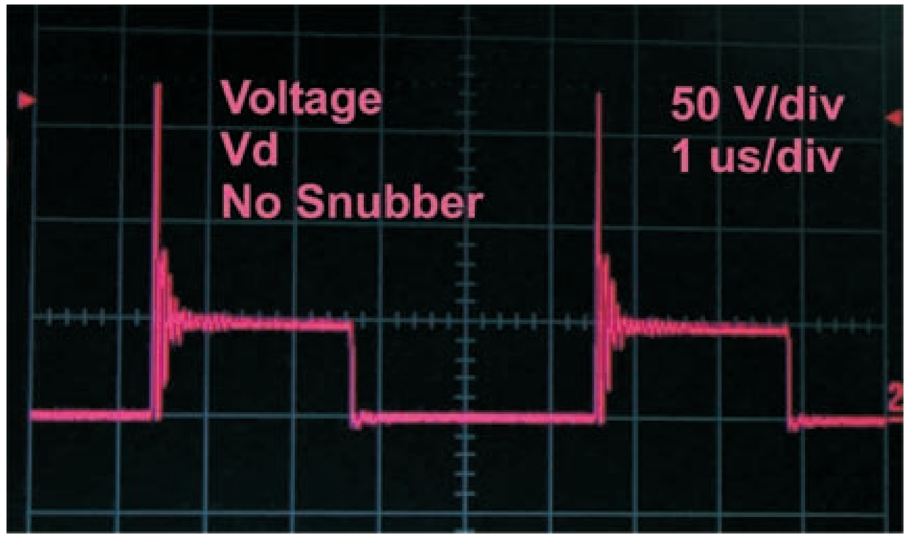

Figure 1: Secondary catch diode voltage waveform, VD, with 100 VAC applied and no snubber

Secondary Catch Diode RCD Clamp Network

A simple RC snubber applied across the catch diode of the converter is not able to sufficiently control the peak of the ringing waveform. Instead, an RCD clamp is used, as shown in the schematic of Figure 2.

RCD clamps are most often applied on the primary of an offline converter where the peak voltage must be tightly regulated to avoid failures. However, they can also be used on converter secondaries, especially when the output voltages. The clamp diode and capacitor must be placed very close to the terminals of the catch diode for maximum effectiveness.

Figure 3 shows the effectiveness of a well-designed RCD clamp. The peak voltage is reduced to 90 V from 175 V.

Design of the components is quite straightforward. The capacitor is chosen so that it retains a relatively constant voltage over each switching cycle. A 600 V multilayer ceramic capacitor was used with a value of 68nF.

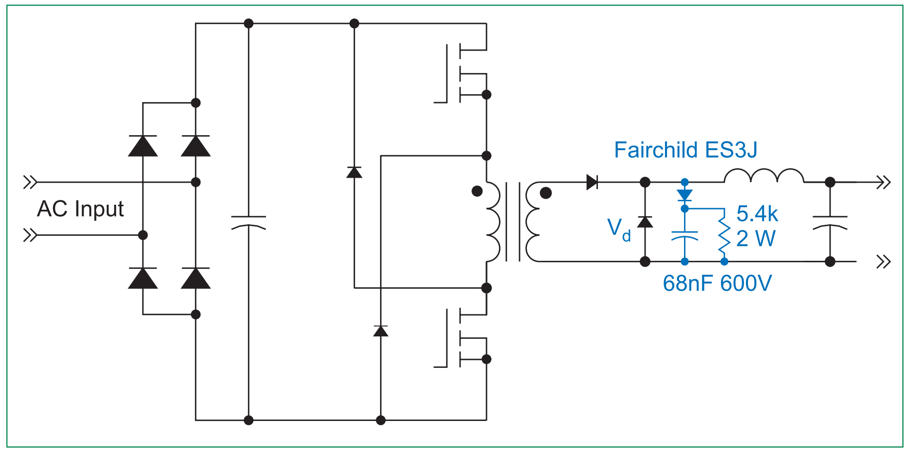

Figure 2: Schematic showing location of Secondary RCD clamp. Only one of the three outputs is shown for clarity.

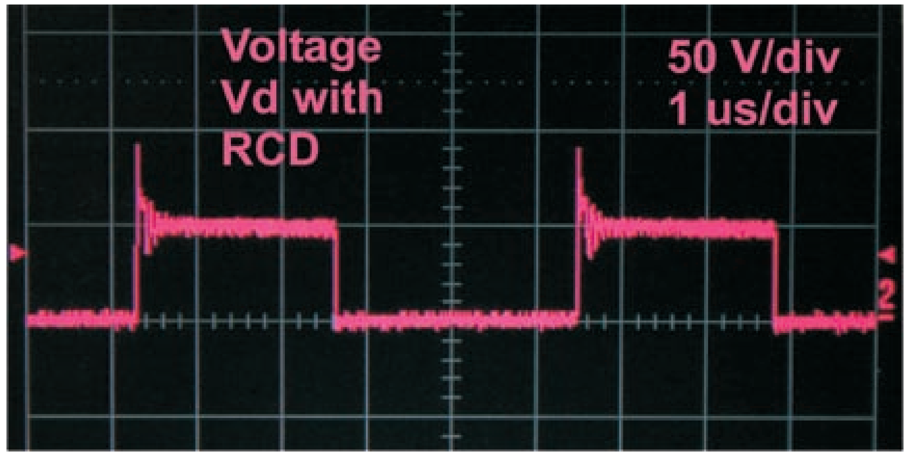

Figure 3: Secondary catch diode voltage waveform with 100 VAC applied and with RCD clamp

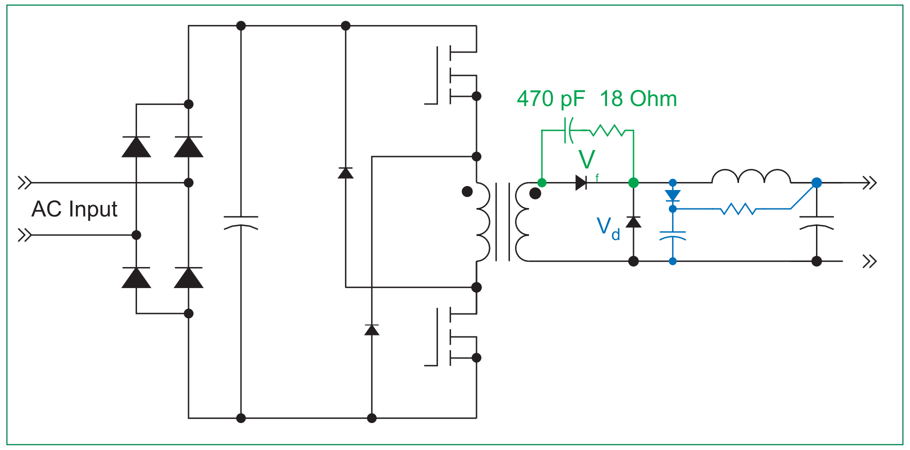

Figure 4: Schematic Showing Improved RCD clamp with lower dissipation, and RC Snubber added to protect the forward diode.

The diode of the clamp needs to be either a schottky, or a fast recovery type. In this converter, a Fairchild 3A ultrafast diode with a rating of 600 V was used (ES3J).

The value of the RCD resistor can be selected according to the process in [2], or can be chosen experimentally. The smaller the value of the resistor, the harder the voltage across the diode is clamped, at the expense of higher dissipation. Full analysis of the RCD snubber can be found in [2]. Although this article is specifically for the flyback converter, the procedure is the same.

The power dissipation in the RCD clamp can be reduced by connecting the resistor to the output voltage, instead of ground, as shown in Figure 4. Depending on the topology used, this can result in significant power savings. For the two-switch forward, approximately 40% of the energy is recovered at low line with this alternate connection. With this approach, the RCD clamp dissipates just above 1 W when the power supply operates at an output of around 400 W.

For very high power converters, you may also consider using a switching converter to discharge the clamp voltage. Active clamp networks can also be used but these add complexity and are beyond the scope of this article.

Secondary Forward Diode Waveform

The RCD clamp only protects the catch diode of the forward converter. It is also necessary to add a snubber across the forward diode on each of the converter outputs. Figure 5 shows the waveform across the forward diode before a snubber is added. The peak voltage spike seen is approximately twice the square wave value. A simple RC snubber is sufficient to reduce this spike to safe levels, as shown in Figure 6. The RC network is placed directly across the forward diode, as shown in Figure 4. The design process for these components is given in [2].

The design of the RCD clamp and the RC snubber must be replicated on the second main output of the power supply. The lower power outputs can usually be designed with RC snubbers only. However, it is important that even the lowest output power diodes be checked for ringing and properly protected if you want to maximize the reliability of your converter.

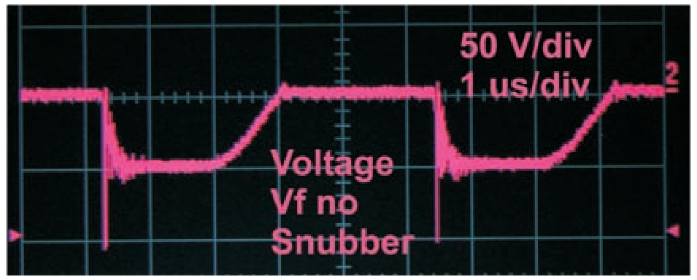

Figure 5: Secondary forward diode voltage waveform with 100 VAC applied and no snubber

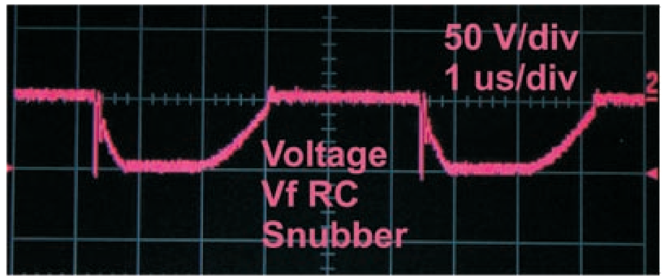

Figure 6: Secondary forward diode voltage waveform with 100 VAC applied and RC snubber.

Summary

The diodes on the output of the forward converter are protected with a combination of RCD clamps, and RC snubbers. It is important that every power diode be protected with a snubber or clamp, and tested under all conditions to ensure that the peak voltage ratings of all devices are never exceeded.

So far, the power stage testing has followed this order:

1、Check gate drive circuit waveforms. A

2、Test primary circuit with resistive load.

3、Insert magnetics into circuit and verify low-voltage waveforms.

4、Design proper voltage clamps on primary switches.

5、Design proper voltage clamps and snubbers for secondary diodes.

All testing has been carried out at a relatively low input voltage – just 40% of the rated input. Before higher voltage testing is done, the overcurrent protection of the power supply must be thoroughly tested. This will be the topic of the next article in this series.

References

1. "Power Supply Development Diary Part IV", Ray Ridley, Power Systems Design Magazine, June 2010.

2. "Flyback converter snubber design", Ray Ridley, Switching Power Magazine, 2005. www.switchingpowermagazine.com

www.ridleyengineering.com

Driving on Solar Panels

An innovative way forward to clean energy

I had the pleasure to talk with Scott Brusaw, an inventor and passionate advocate of clean energy, based in Idaho. He unfolded his mission to develop a road system that would not only utilize the power of the sun to provide enough power to become 100% clean in energy terms (no more coal or oil), but would also be cost competitive against the rocketing cost of construction materials for highways.

Reported by Cliff Keys, Editorial Director, PSD

Scott Brusaw is a man with a clear mission. He wants to help the U.S. to utilize the power of the sun to rid his homeland of the scourge of fossil based energy. As an inventor, he is also an engineer, so therefore logical and practical in his approach. He and his team have developed a solar road module that can collect and route energy intelligently along the U.S. highways.

The Obama administration has now made a request that sidewalks should be utilized to be self funding in terms of 'giving back' energy to redeem the high costs in providing them. Scott's project had already started, but the project was deemed important enough to gain funding from the government for further prototype development.

But who can ever imagine driving on glass? Scott has worked with experts at the top Universities in America and has established that glass can be made cost-effectively with the optical and all the necessary traction capabilities comparable to asphalt required for a tough, durable, cost-competitive roadway system that can collect and route energy from the sun to industry and households alike.

When asked just how much power can be expected from a one-mile (1.61km) stretch of road, Scott explained, "One mile = 5280 feet. Our Solar Road Panels

Imagine a road constructed of solar panels. Scott Brusaw is convinced this could be the way forward to energy independence.

Scott Brusaw pictured with a prototype road panel

are 12 feet by 12 feet (3.66 x 3.66m). Therefore, it will take 5280/12 = 440 panels to create one mile (one lane, 12 feet wide). Each panel is expected to produce 7600Wh of electricity daily based on 15% efficiency and four hours

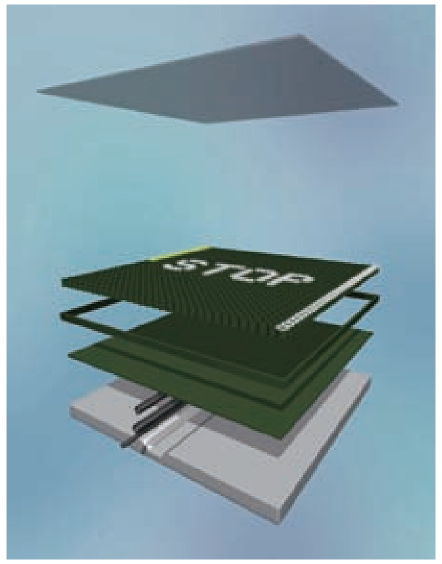

Cross sectional view of the road module prototype

of sunlight per day.

Thus, 440 x 7600Wh = 3.344MWhr per lane per mile. So a typical four lane highway will produce 13.376MWhr per mile, based on four hours of sunlight per day.

According to a 2007 study by the U.S. Energy Information Administration, the average American home used 936kWh per month. Dividing this number by 30 will give an average need of 31.2kWh per day. Dividing this number into the 13.376MWhr per mile, gives us approximately 428. That's how many American homes can go "off-grid" for every mile of 4-lane Solar Roadway. We can wean ourselves off coal. Again, that's based on four hours of sunlight per day."

Scott's company is not publicly traded. He concluded, "We have (or can hire) the technical expertise to make the Solar Roadways a reality. We've received some government funding, but we're always open to a local angel investor who would like to become a part of this project and get his/her hands dirty. We're not interested in someone who's 'just in it for the money', but someone who sees the vision and, like us, wants to leave the world a better place than when we entered it."

There is a great deal more to this project than we have room for in this issue, but I look forward to working with Scott and his team on a full length technical article for a future issue. More information is available through the following (highly recommended) links:

New YERT video:
http://www.youtube.com/watch?v=Ep4L18zOEYI
Scott's TEDx Talk:
http://www.tedxsacramento.com/videos/
Solar Roadways website (contains contact information):
http://www.solarroadways.com

PSDE Green Power
ENERGY EFFICIENCY

Powering CAN

ISO 11898-compliant HS-CAN communication from a high-speed CAN transceiver supplied by a charge-pump

Charge pumps are often the best choice for powering a CAN-bus application that requires a combination of low-power, low-voltage operation and low cost. This article explains how to supply a high-speed CAN transceiver, via a charge pump, to achieve a 5V rail that is required for most transceivers to deliver ISO 11898-compliant communication in automotive electronic control units (ECUs) that only have a 3.3V supply available. The article also discusses the impact on electromagnetic emissions and immunity.

By Robert Regensburger, Senior Member of the Technical Staff, Applications, Maxim Integrated Products Inc., Munich, Germany

Over the past several decades the automotive industry witnessed a rising demand for more comfort, efficiency, and environmental cleanliness, and a growing expectation for better performance and safer vehicles. As a result of these trends, the number of electronic subsystems in a car and the wiring to connect all of them was increasing significantly. With more wire, there was more weight to the vehicle and, of course, more cost. However, in the early 1980s Bosch developed the CAN-bus network, which has now been widely adopted by the auto industry since the bus network offers many advantages including reductions in wiring harness complexity, weight, and cost.

The transition from a centralized control system to distributed systems in automobiles helped the automotive manufacturers meet their goal of reducing the weight and cost of a vehicle. A centralized control system has all actuators, sensors, and switches connected to it through multiple wires. A distributed system locates the electronic control units (ECUs) wherever they are needed – intercommunication connections are made through a bus system (e.g. the two wire CAN-bus network) (Figure 1).

A CAN implementation consists of multiple transceiver modules linked by a pair of bus wires. In each module is a CAN transceiver that provides the physical layer interconnection between the protocol controller (a microcontroller, state machine or other processing engine in the module) and the physical medium (the wires). This new CAN-bus design approach quickly needed to be standardized to ensure proper communication among different suppliers' ECUs. This standardization was first done in 1993 by the ISO (International Organization for Standardization). In 2003 and 2007 further revisions followed, and now the ISO

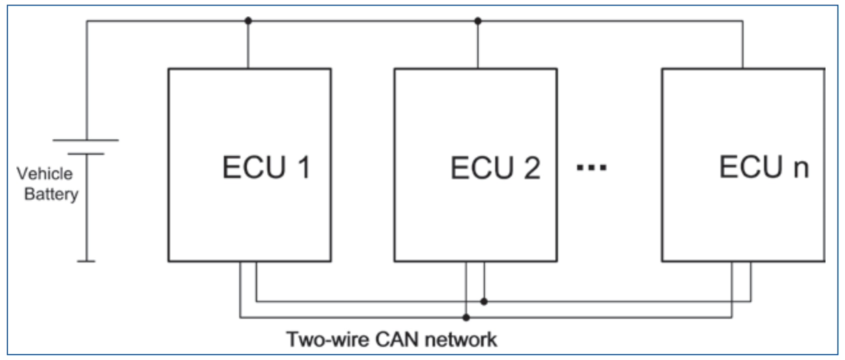

Figure 1: This simplified distributed electronic control unit (ECU) architecture example uses the two-wire CAN network bus to provide communications between ECUs

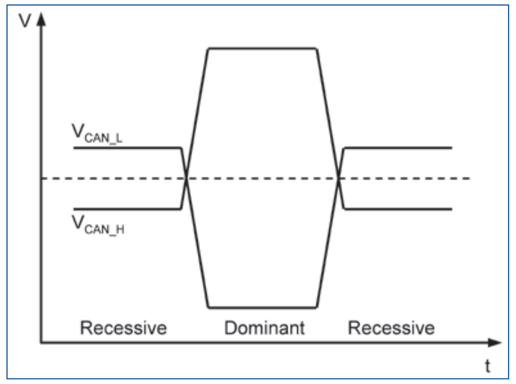

Figure 2: Voltage level of the CAN bus for recessive and dominant logic states

COVER STORY

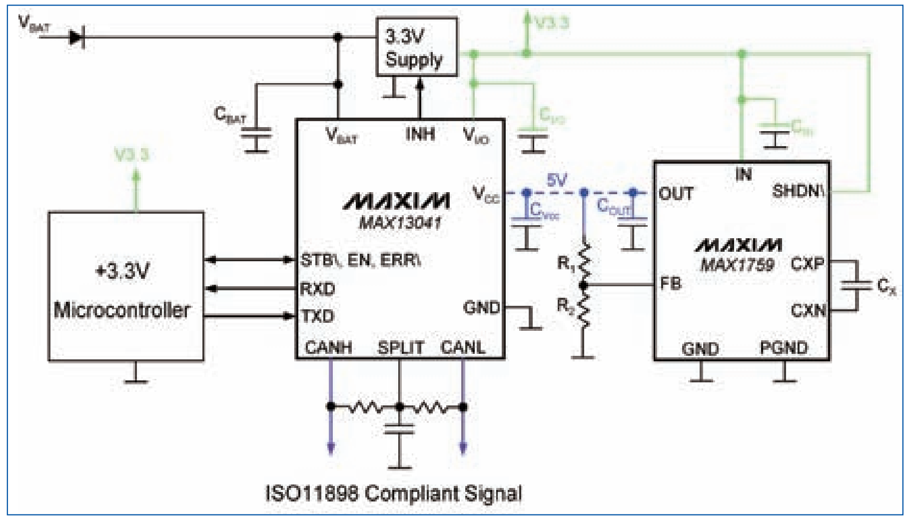

Figure 3: In this circuit, the MAX1759 charge pump supplies 5V to the MAX13041 HS CAN transceiver

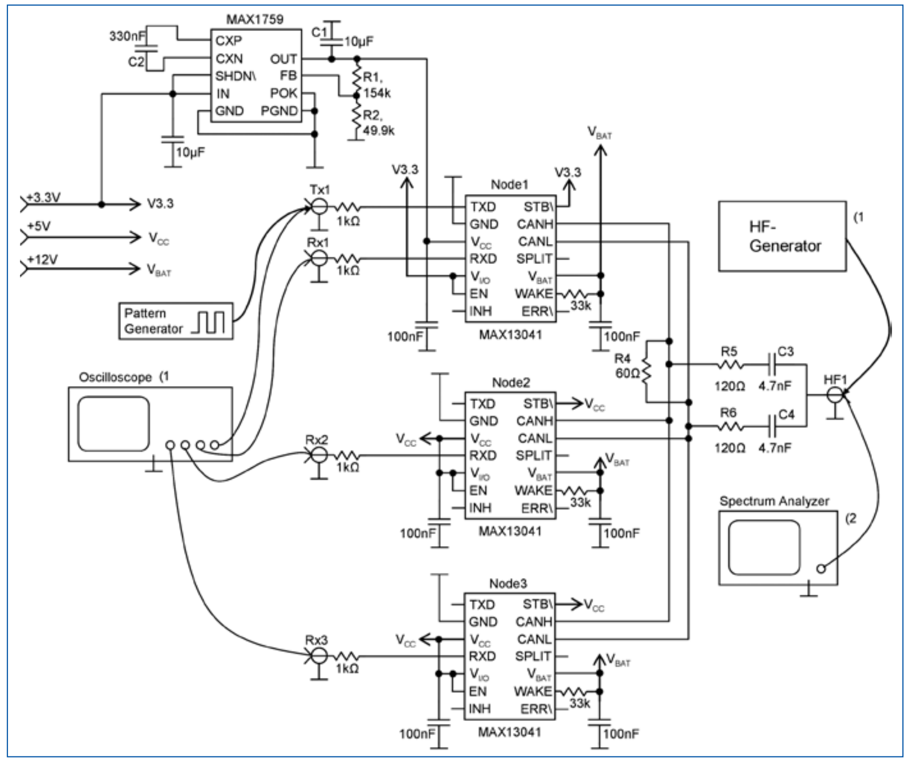

Figure 4: Test setup for DPI and emissions testing
1) The oscilloscope is used for immunity testing only
2) The spectrum analyzer is used for emissions testing only

11898 standard is the defacto standard, accepted by all original equipment manufacturers (OEMs) for all CAN communication in a vehicle.

To be compliant with the ISO standard and to provide the proper bus level, most CAN transceiver bus drivers should be powered by a 5V supply rail. However, it is common in electronic systems engineering for the main supply rails not to meet the subsystem's power requirements. In these cases, the available power rails are often not directly usable for supplying a CAN transceiver, e.g., there might only be a single 3.3V supply available. Sometimes lack of space prevents inclusion of the optimal number of supplies. In other cases, generating the 5V directly from the battery rail might not be acceptable due to heat dissipation issues, especially in systems that need CAN communication at high battery voltages (e.g., during a double-battery condition in a vehicle or in a 24V truck system).

Voltage converters can generate the desired voltage levels; charge pumps are often the best choice for applications requiring some combination of low power, simplicity, and low cost. Charge pumps are easy to use, because they do not require expensive inductors or additional semiconductors.

Selecting the charge pump Transceiver supplies

There are both simple and highly sophisticated CAN transceivers available today, with some requiring a single supply and others requiring multiple supplies. In order to provide proper interoperability between modules from different ECU suppliers and to deliver ISO 11898-compliant high-speed CAN communications, almost all of them though, require a 5V rail that has a certain maximum tolerance.

Some transceivers are also equipped with a built-in I/O level adapter. By using the supply voltage of the protocol controller (on a separate supply pin of the transceiver), the level adapter ratiometrically scales the I/O levels of the transceiver to the voltage levels of the controller. This allows the transceiver to be directly interfaced to controllers operating on supply voltages lower than 5V without the need for any glue logic.

Transceivers with low-power management that support local and remote wake-up have yet another supply pin. This pin must be permanently supplied by the vehicle battery yet consume very little current. Such a feature is needed by ECUs that must be able to use the high-speed CAN bus even when the ignition key is "off".

For a functional description of all other pins on the CAN transceivers, please refer to the respective data sheet for the device you are considering.

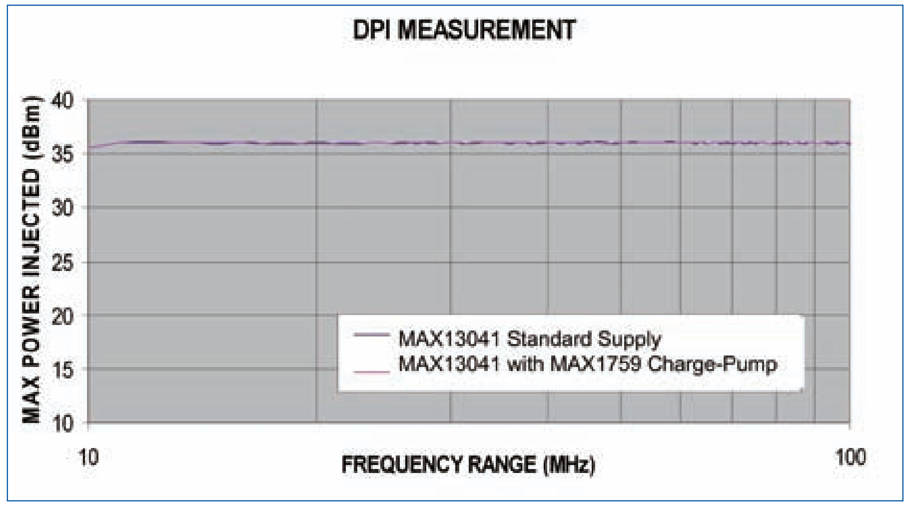

Figure 5: DPI test results

Supply currents

The CAN bus can have one of two logical states: recessive or dominant (Figure 2). In normal communication mode, the transceiver needs it's maximum input current in the dominant state and its minimum in the recessive state. The currents needed for the I/O level adaption and for the remote wake-up capability can be neglected in this case, since they are provided by the microcontroller's supply and the car's battery, and are usually very small.

In the presence of a bus failure, however, the supply current can increase significantly, especially if the CAN_H bus line is shorted to ground. Most transceivers will limit the short-circuit current to a certain maximum value. In order not to risk a breakdown of the supply voltage, it is better to dimension the charge-pump output current for this case.

Taking the above into consideration, supplying a CAN transceiver with the proper power requires a charge pump that features an output voltage of 5V with the voltage tolerance specified in the devices data sheet, and a minimum output current capability to cover the CAN_H short-to-ground event.

Example: Max13041 Transceiver supplied by the MAX1759 Charge Pump

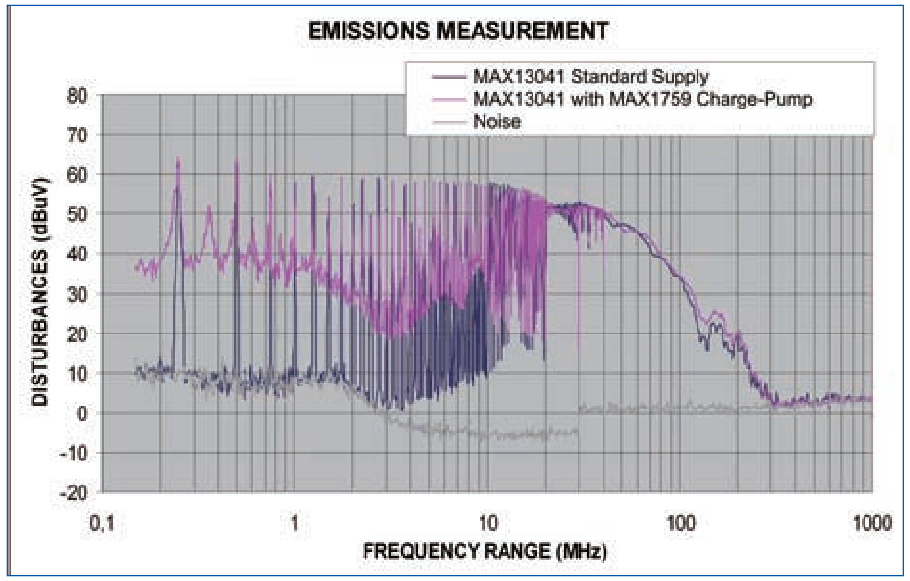

Figure 6: EME curves of the MAX13041 supplied by a standard 5V (blue) and by the MAX1759 charge pump (pink)

Although many conventional CAN transceiver and charge-pump devices are on the market, this article focuses on the MAX13041 HS CAN transceiver and MAX1759 buck/boost regulating charge pump to show how to solve the power-rail issue. The transceiver is supplied through the VCC pin. To provide ISO 11898 standard compliant CAN communication, VCC must be between 4.75V and 5.25V (normal operating-voltage range). This voltage is used to build the proper communication signal between the bus lines (CAN-H, CAN-L), and to supply the receiver stage when the IC is in normal mode.

The transceiver's VI/O input enables the interface with 3.3V I/O microcontrollers so the correct voltage level can be established between the controller's and transceiver's receive/transmit stage (RxD/TxD). The VI/O pin can also be supplied by 5V, of course, when the application is communicating with such a controller.

The VBAT pin (usually connected to the car's 12V battery) supplies power to a very-low-quiescent current wake-up detection circuit. This pin enables the MAX13041 to wake up from sleep mode on a CAN message. For a detailed description of all other pins, please refer to the MAX13041 data sheet.

In normal communication mode, the MAX13041 needs a maximum input current (VCC pin) of 80mA in the dominant state and 10mA in the recessive state (Figure 2, again). The currents into VI/O and VBAT can get neglected. In the presence of a bus failure, the VCC supply current can increase significantly, especially if the CAN_H bus line is shorted to ground. The Max13041 will limit the short-circuit current to IO(SC) = 95mA.

Taking the above into consideration, supplying the CAN transceiver with the proper power requires a charge pump that features an output voltage of 5V with the voltage tolerance mentioned above, and a minimum output current capability of 95mA.

Charge Pump Requirements

The MAX1759's architecture allows the

COVER STORY

input voltage to be higher or lower than the regulated output voltage. However, in this application the charge pump operates as a step-up voltage converter only. When VIN is lower than VOUT, the charge pump operates as a regulated step-up voltage doubler. When lightly loaded, the charge pump switches only as necessary to supply the load, resulting in low quiescent current. Output voltage ripple does not increase with light loads.

For a detailed description of all features of the charge pump, please refer to the MAX1759 data sheet.

Implementing a 3.3V solution

The circuit in Figure 3 illustrates how easy it is to supply the MAX13041 with the charge pump. The MAX1759 is simply added to the VCC input of the CAN transceiver (see the blue dashed line), producing a 5V output voltage with the required tolerance and output current. This configuration allows the rest of the circuitry to be supplied by lower voltages. In this example, an external supply voltage of 3.3V (green) supplies the charge pump (IN), the microcontroller, and the VI/O level-translator voltage of the transceiver. The active-low SHDN input of the charge pump is pulled high, putting the part into it's ON state. The detailed dimensioning of the input/output (CIN, COUT) and the flying capacitor (CX) is described in the MAX1759 data sheet.

Electromagnetic compatibility

Electromagnetic compatibility (EMC) can be a challenge to achieve with CAN applications, especially if they are supplied with a switching voltage regulator. The wiring harness of the CAN system is particularly problematic, as the CAN_H and CAN_L pins of the CAN transceiver are the interface to the bus network running into the entire vehicle. If care is not taken, one can encounter interference, or create interference, that propagates from the CAN supply, through the transceiver, over the bus wires into other ECUs, or into the neighboring cables of the harness. Such interference can cause miscommunication or malfunctioning of the transmitting or other control units in the system.

Because of this concern, we test the EMC behavior of the MAX13041 supplied by the MAX1759 charge pump and compare it to the behavior of the transceiver supplied by a filtered, 5V-supply. In this way we see both the impact of EMC interference from the charge pump and the pump's robustness against interferences from the CAN lines propagating to the supply. In this test, we consider two domains: electromagnetic immunity (EMI) and electromagnetic emission (EME).

Immunity Testing (EMI)

The ISO 11452 specifications describe several methodologies for testing immunity to RF disturbances, including bulk current injection (BCI), transversal electromagnetic-cell (TEM-cell), stripline, and direct power injection (DPI).

We use the DPI method because of its high reproducibility (due to the use of a well-defined test board) and the relatively low test effort needed. The principle of the DPI test is straightforward: inject a certain AC voltage into the bus lines, modulated or not, and check the integrity of the transmitted data signal through the transceiver's RXD pin. This method also facilitates comparison between different suppliers' designs and, moreover, is used by independent laboratories testing CAN transceivers (e.g., IBEE [Ingenieur Buereo fuer industrielle Elektronik]).

Test setup

The test setup (Figure 4) consists of three identical transceivers soldered on a defined PCB, with one transceiver supplied by the MAX1759 charge pump. Node 1 operates as a transmitter for a bit pattern that simulates a CAN message to be received and monitored at the RxD output ports of all transceivers. For RF decoupling of outputs Rx1 to Rx3 and for the input TxD1, 1kΩ resistors are used. A buffer ceramic capacitor (C = 100nF) is used at the supply ports VCC and VBAT of every transceiver IC. The resistors at the wake-up pin have a value of 33kΩ. The devices are set to normal mode by tying the pins EN and the active-low STB high. The VCC voltage for node 1 is generated by the MAX1759 charge-pump circuit, which is supplied with 3.3V. The 3.3V supply was also used as the VI/O voltage of transceiver node 1.

The output capacitor C1 for the charge pump is 10µF; the flying capacitor C2 is 330nF; and the input IN pin is decoupled with a 10µF capacitor. In the test circuit, the bus termination is realized by a central termination using the 60Ω R4 resistor. Symmetrical RF coupling/decoupling is realized with the parallel RC combination of R5/R6 = 120Ω, C3/C4 = 4.7nF. The external 3.3V, 5V, and 12V supplies are provided by standard power supplies, filtered by a filtering network.

Test procedure

The test is performed with the MAX13041 CAN transceivers operating in normal mode. The first test run is done with all transceivers supplied by a standard VCC = 5V supply; at the second test run, one CAN transceiver is supplied by the charge pump (Figure 4). A pattern generator produces a square wave with a duty cycle of 50% to simulate a CAN signal (with permanent data alternation 0-1-0) of 500kbps on the TXD pin of node 1. An HF generator on the RF input (HF1) injects an amplitude-modulated (AM) AC voltage, with a certain frequency, corresponding to a power of 36dBm into the CAN lines to simulate the disturbances.

To evaluate immunity, an oscilloscope is used to compare the Rx signals of the three transceivers in the network while they are under the influence of the disturbances to the signal fed into TXD. A validation mask with a maximum allowed voltage deviation of ±0.9V and a maximum allowed time deviation of ±0.2µs is overlaid across the TXD signal-wave shape.

If the failure criteria is true (i.e., if one of the transceiver's RXD signals is beyond the validation mask window), the injected RF power is reduced by 0.2dBm and the same test (at the particular frequency step) is repeated until the failure criteria is false. Then, the current power value is recorded and the next frequency step is adjusted. The test is carried out over a 10MHz to 100MHz frequency range.

DPI test results

Figure 5 shows the test-result curves of the MAX13041 supplied by a standard 5V supply on VCC (blue) and the MAX13041 supplied by the charge pump (pink). The X axis indicates the frequency range, while the Y axis indicates the maximum power injected without failure.

The blue and the pink lines are almost identical. This indicates that the EMI behavior of the circuit is dominated by the CAN transceiver's EMI susceptibility and not the charge pump's EMI susceptibility. Therefore, supplying the MAX13041 CAN transceiver with the MAX1759 charge pump does not significantly affect circuit performance when the circuit encounters any EMI.

Emissions testing (EME)

The emissions test is performed on the same test board and test setup as the DPI test, except that the power injector (HF generator) is replaced by a spectrum analyzer. The test is again performed with the CAN transceivers operating in normal mode. The first test run is performed with all transceivers supplied by the standard VCC = 5V supply; the second one is performed with one CAN node supplied by the charge pump. The applied square wave on the CAN TXD input (simulating a transmitting bit stream of 500kbps) is maintained, and the emissions on the CAN lines are measured and recorded by the spectrum analyzer in the 100kHz to 1GHz frequency range. The oscilloscope is not required (Figure 4).

Emissions test results

Figure 6 shows the resulting EME curves of the MAX13041 supplied by the standard 5V supply on VCC (blue) and by the MAX1759 charge pump (pink). The X axis indicates the frequency range, while the Y axis indicates the level of the disturbances.

Here the peaks of the blue and the pink lines (one transceiver supplied by the charge pump) are almost identical to the lines for the MAX13041 with the standard 5V supply (blue). This shows that the emissions behavior of the circuit is dominated by the CAN transceiver's emissions compatibility, and not that of the charge pump. These test results indicate that it is possible to supply a CAN transceiver with a charge pump without significantly influencing the overall EMC behavior of the system. However, if transceivers or charge pumps of other semiconductor vendors are selected, it would be wise to run these tests on those specific products since each vendor' s product performance could be different.

Conclusion

It can be challenging to achieve electromagnetic compatibility with CAN applications, especially if they are supplied by switching voltage regulators (charge pumps). However, this article demonstrates that the EMC behavior of the circuit is not significantly influenced by the charge pump. Thus, supplying a CAN transceiver with a charge pump for applications that require low-power, low-voltage operation at low cost is an option for system designers who do not have a readily available 5V power-supply rail.

www.maxim-ic.com

Digital Isolators

Superseding optocouplers in industrial applications

For more than four decades, optocouplers have been the "default" signal isolation device, but CMOS-based digital isolation technology has made available smaller, faster and more reliable solutions that have begun replacing optocouplers in many applications. Both classes of devices must provide signal transmission with galvanic isolation, often in harsh industrial environments and in the presence of strong electromagnetic fields, surges, fast transients and high noise levels.

By Don Alfano, Director of Power Products, Silicon Laboratories Inc

An optocoupler is a hybrid assembly that pairs a forward-biased light-emitting diode (LED) and a photodetector. The LED emits light in response to the incoming signal: the light passes through a transparent, electrically-insulating film or dielectric, and the detector recovers the signal and presents it at the output pins.

The digital isolator's basic operation is similar to that of the optocoupler, except an RF signal replaces the emitted light. For example, Silicon Labs' digital isolator IC consists of two identical semiconductor die connected to form an RF transmitter and receiver separated by a differential isolation barrier. Data is transferred from input to output using simple on/off keying. When VIN is high, the RF carrier is transmitted across the isolation barrier. The receiver asserts logic 1 on VOUT when sufficient in-band carrier energy is detected.

In an optocoupler (Figure 1a), the LED and output die are attached to a split lead frame and separated by a physical gap containing a transparent shield that reduces parasitic input/output coupling capacitance. Optocoupler cost and complexity increases with channel count, and isolation breakdown voltage is primarily determined by the package plastic mould compound.

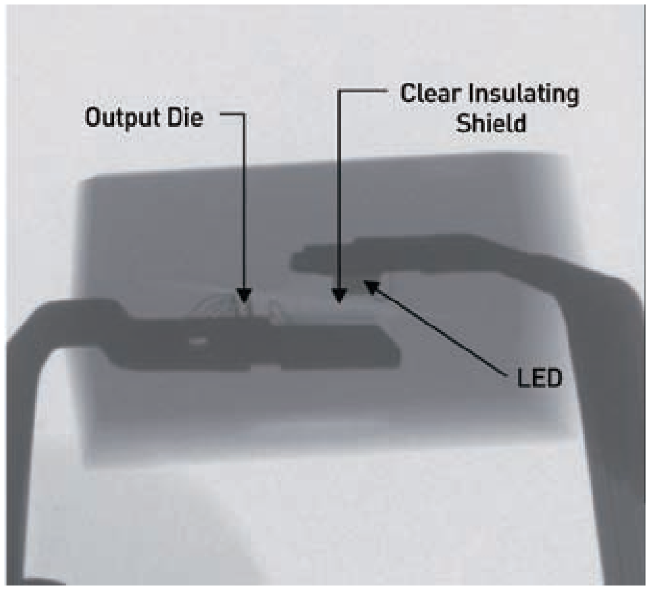

Figure 1a: Optocoupler assembly X-ray

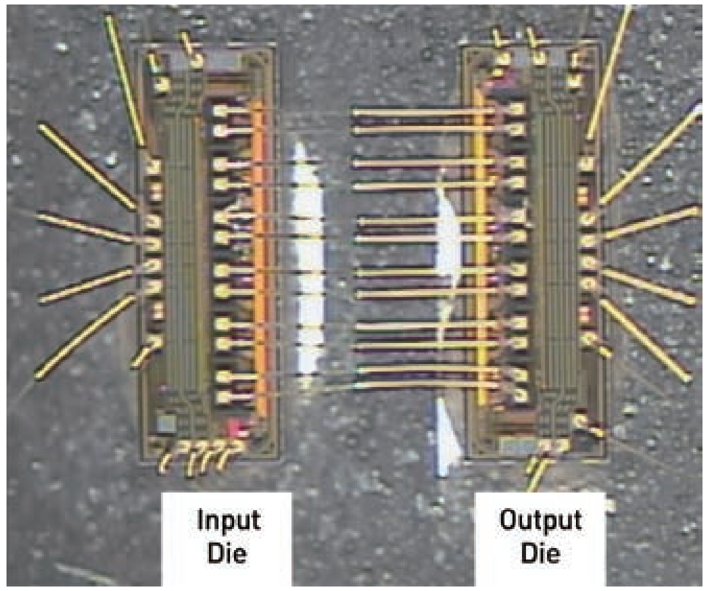

Figure 1b: Decapsulated 6-channel digital Isolator

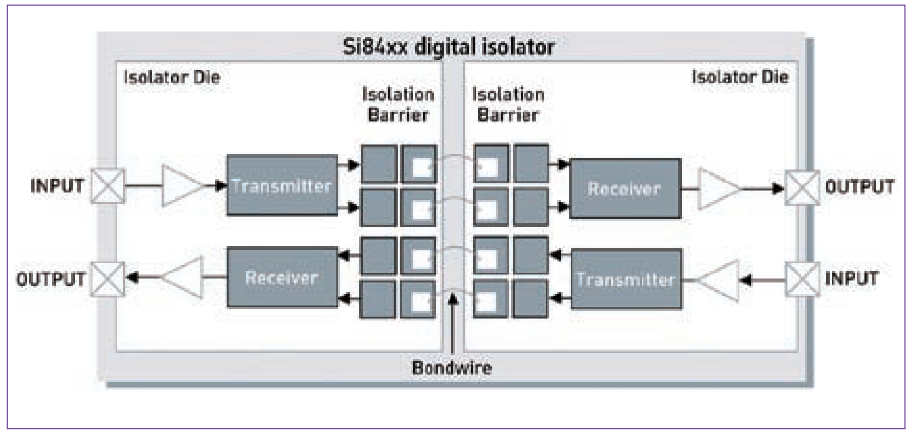

Figure 2: The digital isolator's capacitive-isolated signal path is fully differential for maximum common-mode rejection

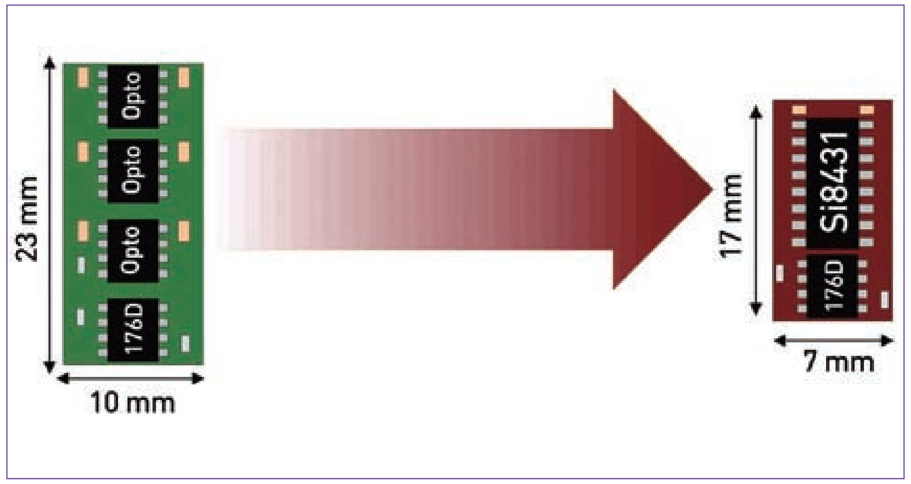

Figure 3: Profibus optocoupler implementation vs. digital isolator

The 6-channel digital isolator (Figure 1b) contains two die fabricated in standard CMOS technology in standard IC packaging. Each die contains six isolator channels (transmitter, differential isolation barrier, and receiver circuit) and forms six complete isolator channels when connected. Unlike the optocoupler, the digital isolator channels occupy a very small die area, enabling cost-effective, high-channel-count isolation solutions.

Safety standards

Isolators must meet safety standards for robust galvanic isolation and be reliable enough to outlast the equipment in which they are installed. The designer must consider operating parameters such as common-mode transient immunity (CMTI), key timing parameters, and noise immunity characteristics such as EMI and RF susceptibility, and reliability concerns such as continuous working voltage and mean time-to-failure (MTTF). Safety insulation is the most critical aspect of an isolator, and insulation must be uniform; uniformity is a function of the insulator material and the fabrication process.

The dielectric strength of an optocoupler's plastic package compound can vary by as much as 300% due to voids created during fabrication. Silicon Labs' digital isolators use semiconductor oxide layers, fabricated by standard CMOS techniques, for the primary insulator. The oxide deposition process is highly uniform and has a dielectric strength variation of only 20 percent. The result is a higher absolute maximum breakdown voltage in a substantially smaller size compared to optocouplers and insulator reliability that is independent of the packaging process.

Isolators may be classified as "basic" or "reinforced"; distinctions between the two categories include the voltage that each must withstand for one minute in 100% safety testing (2.5 and

Product	Channels	Operating Temp Range (Deg. C)	Supply Voltage (V)	Max Supply Current (input + output) (mA)	Max Prop Delay Time (ns)	Minimum Pulse Width (ns)	Maximum Data Rate (Mbps)	Pulse Width Distortion (ns)	Prop Delay Skew (ns)	Output Rise Time (ns)	Output Fall Time (ns)	Channel-to-Channel Skew (ns)
digital isolator	4	-40 to +125	2.7 to 5.5	7	10	6	150	1.5	2	4	4	0.5
Optocoupler	1	-40 to +85	4.5 to 5.5	17.5	22	20	50	2	16	8	6	20

Table 1: Operating characteristics of a 50Mbps optocoupler compared to a digital isolator

5kVAC respectively) and the minimum “creep” path length that their construction must provide.

Operating conditions

Optocouplers require current to bias the LED and some form of bias on the output side, and these currents vary widely with the type of optocoupler. The optocoupler’s power consumption increases with LED forward current, which can range from 1mA to over 15mA and may require an external driver. The optocoupler output impedance can be low or high depending on its architecture. Most low-cost optocouplers have a simple transistor output that is high-impedance when LED forward current is at zero and lower impedance at higher LED currents. Other (usually higher speed) optocouplers have an active photo coupler and output driver that requires an external bias voltage. Such devices have low output impedance but increase total operating current to 15mA to over 40mA.

The digital isolator offers significantly higher operating efficiency (1.7mA/channel at 10Mbps, VDD=5V, CL= 15pF) compared to an optocoupler solution. Its high-impedance input consumes microamps of leakage, and its 50Ω CMOS output driver can source or sink 4mA. The digital isolator’s power dissipation rises linearly with increasing data rate, but at a much slower rate than that of a typical optocoupler.

Optocoupler timing parameters can change with three variables: LED wear-out, LED current and operating temperature. As a diode ages, LED light output (LOP) diminishes, impacting timing and impedance characteristics. LOP also falls with increasing temperature. LOP degradation is partially related to LED current, and the system designer must take into account the effects on LOP when deciding the LED operating range, trading off drive current for life expectancy and CMTI performance.

Timing specifications are significant for many digital isolator applications. For example, the digital isolator exhibits propagation delay (Tpd) that is not only very nearly constant across its operating temperature range but is substantially less than that of typical optoisolators. Tpd for optoisolators varies inversely with drive current, increases with temperature, and is also different for rising and falling signal edges. The digital isolator’s rise and fall times vary by only 1ns across temperature and supply voltage, and worst-case propagation time is approximately 9ns at 120°C.

Low-capacitance design

Low parasitic capacitances are inherent in the construction of digital isolators, but difficult to achieve in an optocoupler. The designer must deal with this fact when considering tolerance to common-mode transients. If fast changes in common-mode voltages are anticipated, bias currents must be set to ensure that the LED cannot be momentarily activated in error. Inadvertent LED activation can impact power consumption and service life. With an input-to-output capacitance of just 100fF (femtoFarads), the noise immunity performance of a digital isolator is expressed in a minimum CMTI of 25kV/sec. The structure is likewise very tolerant of incident radiated electromagnetic interference (EMI). The fully-differential signal path rejects almost all interfering signals induced in it, while the small physical size of the isolating capacitors and the design of the low-power main oscillator also contribute to meeting the demands of the FCC Class B Part 15 test regime.

Digital isolators are designed to tolerate operation in close proximity to large electric motors and other magnetic field sources. For example, the magnetic field immunity of a Silicon Labs digital isolator has been assessed as withstanding magnetic fields of at least 1000A/meter (per IEC 61000-4-8 and IEC 61000-4-9 specifications), which is far in excess of that likely to be encountered in an operating environment. Similarly, the device can offer higher electrostatic discharge (ESD) immunity than most optocouplers. Once installed in a board, the isolator becomes part of a larger circuit where handling-related ESD hits are often diffused across lower impedance circuit paths. As a result, an isolator with a 4kV ESD rating can reliably operate within a system having an ESD event of 15kV. Standard system-level design procedures to guard against transients and noise should always be observed. The device itself needs no external components other than a small bypass capacitor (0.22 to 1μF) on the supply rail to each (internal) chip. It is as easy to use as connecting a standard CMOS gate.

Illustrating the typical gains designers can achieve by switching from optical to RF isolation techniques, Figure 3 depicts the PCB area required to implement a Profibus interface. Profibus is an industrial serial communication standard that uses a twisted-pair serial link. It is similar to RS-485 or RS-422 and can operate in either a low-speed (1.5Mbps) or high-speed (12Mbps) mode. In this case the line interface chip is a 75ALS176D differential bus transceiver. To interface it to system logic with isolation requires three separate optocouplers (for receive, transmit and transmit-enable signals), as well as a number of passive components. The digital isolator package accommodates all three signal paths (with capacity to spare) and connects directly to system logic and to the ‘176D with no need for bias or other components.

Summary

While optocouplers have been the dominant signal isolation device for many years, the advent of the digital isolator gives designers a smaller, more integrated, faster and lower power alternative with none of the stability or wear-out mechanisms of optocouplers.

www.silabs.com

Integrated Driving

IGBT gate driver for automotive power inverters

Its more than 10 years since the market introduction of Avago technologies first smart gate driver. At that time it was the world's first integrated IGBT gate driver optocoupler with inbuilt fault detection and feedback functionality. The use of DESAT fault protection techniques was well known even then, but the complex circuit nature and high associated cost, marginalized its use to a very small market segment.

By Patrick Sullivan, R&D Engineer, Isolation Products Division, Avago, Boeblingen, Germany

The introduction of this integrated gate driver was a major milestone, in that it enabled adoption of high performance IGBT protection on a mass scale, in medium and low power inverter industrial applications.

Inverter drive technology has now moved into the automotive realm, with applications ranging from low power applications such as air conditioning and heating, through to high power applications such as traction in Hybrid and full electric vehicles.

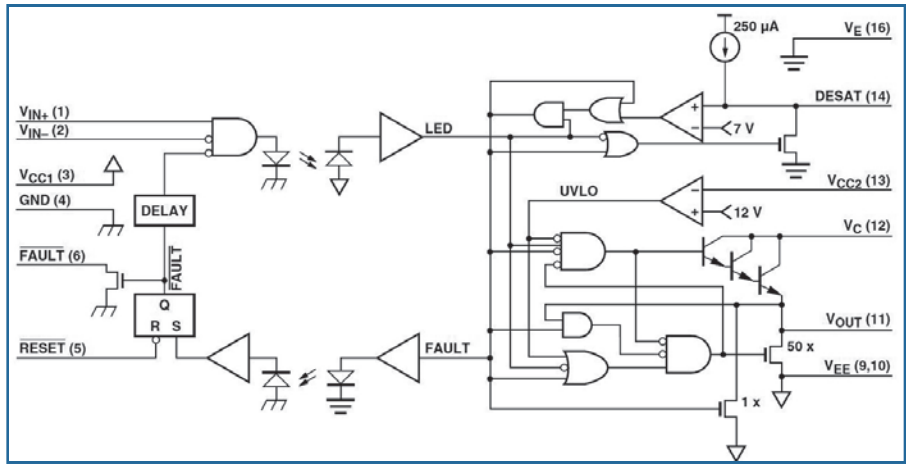

Figure 1: ACPL-36JV Functional Diagram

IGBT Short Circuit Robustness

Although many new types of power switches are being evaluated for use in automotive inverters such as silicon carbide, the current preferred power switch in high voltage inverter applications is the IGBT.

In the desire to minimize power losses in IGBT's, subsequently generations of IGBTs have sought to reduce both switching and conduction losses.

In regards to conduction losses, often a compromise is made with robustness.

A reduction in conduction loss often leads to an increase in short circuit current and consequently a reduction in short circuit survival time.

So to achieve the requirement of low conduction loss and maintain overall system robustness, it is important to have a fast and reliable IGBT short circuit detection and protection circuit.

IGBT Fault Detection Methods

Many types of internal or external fault conditions in an inverter can result in current overload conditions in one or more IGBTs; examples are phase to phase short circuit's or shoot conditions on inverter bridge legs. Some of these faults can be detected using phase current sensors, but not all faults may be detected in this manner.

The alternative to using the phase current measurement method is to detect the current level at each IGBT. There are several methods of detecting the current level e.g. shunt resistor or split emitter IGBT. Each of these methods generates a voltage signal which is proportional to the load current on the IGBT.

The over current protection method in turn uses this voltage threshold to trigger protection mechanisms. Since the maximum tolerable current for the IGBT is dependent on IGBT process variations, operating temperature and gate voltage it is necessary to set the trigger threshold at quite a conservative level.

DESAT detection as it names suggests relies on directly detecting the IGBT coming out of saturation due to an over current condition. The advantage of this method is that it monitors the actual operating condition of the IGBT and effectively reduces the influence of many external factors, enabling higher power utilization of the IGBT.

Integrated Gate Driver Functionality

The ACPL-36JV incorporates all the necessary features to provide an automotive grade integrated isolated IGBT driver with DESAT fault detection. High speed bi-directional communication is

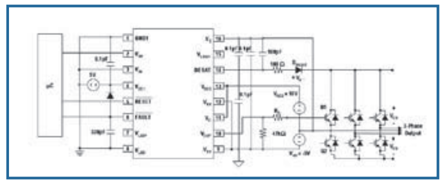

Figure 2: IGBT Application Circuit

achieved by two high speed optical links between two integrated circuits, buffer IC1 and output IC2.

The buffer IC which is gnd referenced to the low voltage controller is used to transmit the isolated gate drive trigger signal and acts as a receiver for the fault status signal.

The output IC is based on a BiCMOS/ power DMOS process providing a high performance gate drive circuit drive together with fault detection circuitry.

Fault Management

Just as important as the detection of the fault is the fault resolution.

By the time the fault condition is detected, it is possible that quite a considerable current is flowing. So if the IGBT is shut of very quickly, the fast di/dt together with unavoidable parasitic connection inductance can potentially cause the peak voltage rating to be exceeded, defeating the protection philosophy.

This problem is mitigated by implementing soft shut turn off, which reduces the di/dt by increasing the IGBT gate discharge time in the event of a fault condition. The autonomous fault detection function can be configured to simultaneously shut down all other gate drivers at the same time. Alternatively the fault detection may be configured to isolate fault detection and signaling to each IGBT separately. The later method readily allows the implementation of a graceful fault and shutdown strategy which is often desirable in automotive traction applications.

Reliability

Automotive quality and reliability expectations are typical much higher than many consumer application and industrial applications.

This increased level of reliability often has to been obtained in a more hostile environment.

One of the key elements of the optically isolated gate driver is the internal LED.

The last decade has seen rapid advances in the performance of LED technologies, enabling their use in an ever expanding range of illumination applications.

These same technological advancements have also enabled significant improvements in LED's for optocouplers.

The purpose designed LED used in all of Avago's automotive optocoupler products offers not only excellent stability over a wide temperature range, but also an extremely stable operation even after long periods of time at high ambient temperatures.

The gate drive and fault detection functionality must operate flawlessly even in the presence of high levels of radiated and conducted electromagnetic noise.

Such noise emissions have a high propensity to cause disruption to low voltage digital signals. Occasional false triggering of the fault detection signal might be regarded more as an annoyance, but false triggering of the IGBT gate driver could result in uncontrolled shoot through in inverter legs, leading to either immediate or latent IGBT damage.

In the case of immunity to radiated emissions the advantage of optical transmission technologies is perhaps obvious, but less obvious is the advantage in regard to common mode voltage immunity. Optical isolation allows the internal separation distance to be large; ensuring a very low parasitic capacitor across the insulation boundary. Secondly the beauty of optical transmission technology is that the data transmission modulation frequency (light) is many orders of magnitude higher than external noise frequencies, enabling the use of a highly efficient optical transparent faraday shield on the receiver. One

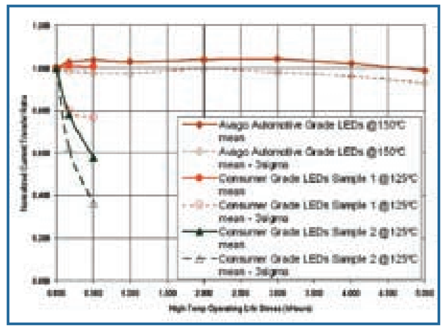

Figure 3: Optocoupler LED High Temperature Lifetime

of the fundamental requirements of the isolated gate driver is to provide high voltage level shifting functionality.

The peak voltage stress applied across the optocoupler is directly related to the DC link voltage. Many traction applications today are using 400V link voltages but in the near future this will increase to 900V. Very early adopters of inverter drives often observed, that compared to 50Hz AC the increased HV stress of a high frequency inverter was often found to cause premature insulation failures in the winding insulation of order generation AC induction motors.

This same extreme HV stress condition is also observed across the isolation of the gate driver. To prevent the activation of wear out mechanisms such as partial discharge, space charge degradation and other time dependent aging mechanisms, thick double insulation polymer construction is used. Ensuring that maximum E-field stress levels are always maintained at long term sustainable levels. An additional benefit of such a construction is the ability to meet reinforced or double insulation requirements for safe insulation applications.

In addition to designed in reliability. Consideration needs to be given to quality control procedures such as TS 16949 and qualification testing according toAEC-Q100. This includes qualification and testing at multitude of levels, ranging from design rules and foundry level through to packaging.

www.avagotech.com/optocouplers
www.avagotech.com

Special Report – Automotive Electronics

Current Sensing in HEVs

Advances in Hall effect current sensor technology

Consumers are embracing environmentally friendly "green cars" as a result of the rising cost of fossil fuels and a growing concern for the health of the environment. Sales forecasts have predicted that green car sales will comprise 20%-25% of all vehicle sales by the year 2015. The hybrid electric vehicle (HEV) is quickly becoming the most popular green car and by 2015 is expected to comprise approximately 12% of global vehicle sales.

By Shaun Milano and Mike Doogue, Product Marketing, Allegro MicroSystems, Inc

Hybrid electric vehicles employ complex power electronic circuitry to control the flow of electric energy throughout the vehicle. In a single motor HEV (see figure 1) the motor acts as a drive motor in parallel with the internal combustion engine, or as a generator to charge the battery during regenerative braking.

A typical HEV contains various systems that require electrical current sensors for maximally efficient operation; including AC motor and DC-DC converter applications. This article focuses on recent advances in Hall effect current sensor technology and the use of unique, high bandwidth, enhanced resolution current sensors in HEV applications.

The HEV power cycle

In the HEV power cycle the main battery voltage is inverted as shown in Figure 1 and the resulting AC voltage is applied to the motor which in turn drives the wheels. During regenerative braking the AC motor also serves as a generator. When the regeneration system is active, the output of the motor/generator is rectified and converted to a DC voltage necessary to charge the HEV battery cells, completing the power cycle. If the HEV is a plug-in vehicle, then line voltage can also be rectified and used to charge the battery.

The regenerative braking process is a primary contributor to the improved fuel efficiency of an HEV, since braking energy which is normally wasted in the form of heat is partially recovered and used to charge the main battery. To power the low voltage infotainment and body control subsystems in the car a DC-DC converter is typically used to reduce the hybrid battery voltage (typically 300 to 500V) to a lower level DC voltage.

A Revolution in Hall Effect current sensing

One drawback of conventional Hall effect sensors, when used in current

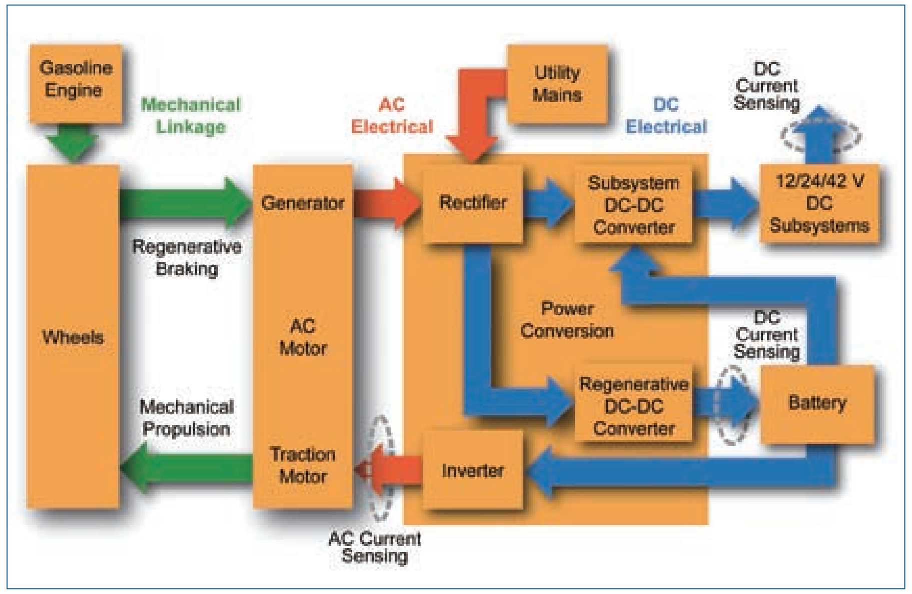

Figure 1: Typical HEV system block diagram

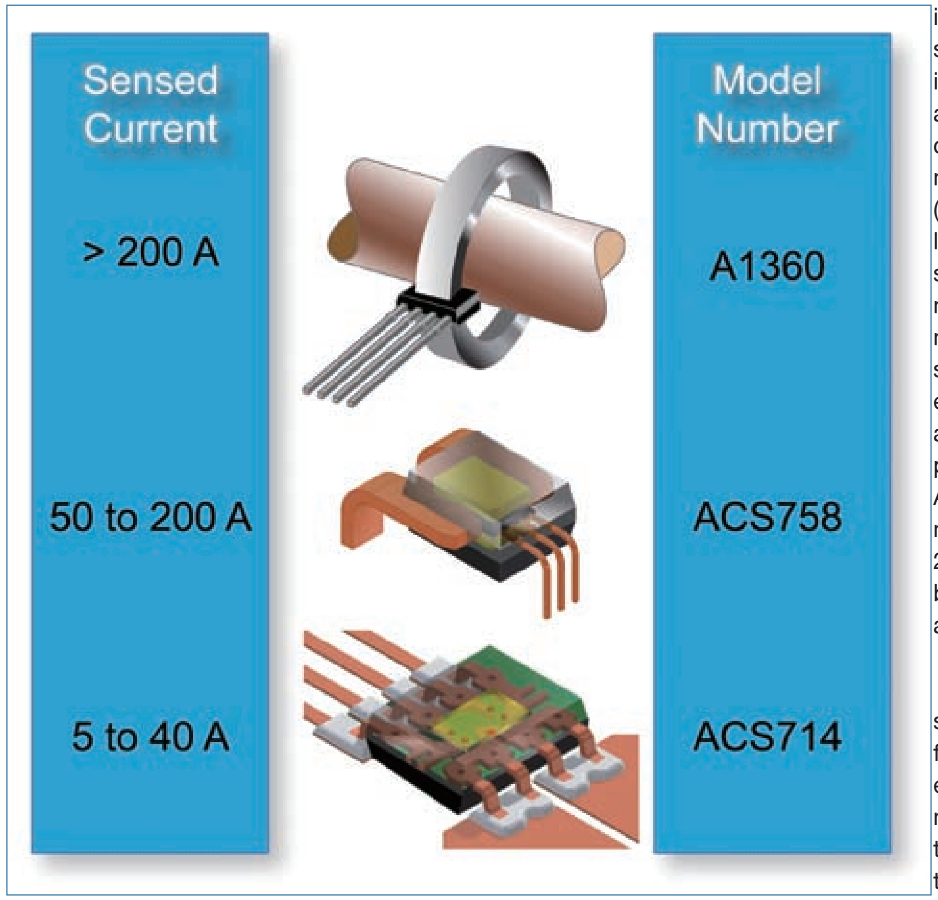

Figure 2 depicts the wide range of proprietary package configurations in the Allegro current sensor family and displays the current magnitude that can be sensed using each package type.

sensing applications, has been a general limitation in both accuracy and output signal bandwidth. However, Allegro ® MicroSystems, Inc. has developed a broad family of Hall effect current sensor integrated circuits (ICs) that are ideally suited for HEV applications.

The features and benefits of these industry leading Allegro current sensors include:

- Signal processing and package design innovations enable > 120kHz output bandwidth
- The highest current resolution, lowest noise spectral density Hall sensors in the marketplace
- Proprietary, small footprint sensor packages with galvanic iso lation
- Reduced power loss: through hole compliant and low-resistance integrated conductor packages
- Precise factory programming of sensor gain and offset

Current sensing in inverter applications

The 3-phase, full bridge driver in a typical inverter converts DC battery voltage to a 3-phase AC voltage that is required for efficient operation of the system motor (see Figure 3b). The inverter phase currents are measured and the resulting information is typically used to control the pulse-width modulated (PWM) inverter switches (typically IGBTs). The inverter control loop requires high bandwidth current sensors to improve accuracy, and to maximize motor torque and overall motor efficiency. High side current sensors with fast response times also enable over-current protection during a short circuit condition from a motor phase to the system ground node. The Allegro A1360 Hall linear device is tailor made to meet the voltage isolation, > 200 ampere (A) load current, and high bandwidth demands of HEV inverter applications.

The A1360 linear Hall effect sensor is typically placed in the gap of a ferromagnetic toroid which surrounds each inverter phase conductor in the motor (Figure 2). As current flows in the conductor the toroid concentrates the resulting magnetic field through the standard single-in line package (SIP). The A1360 Hall transducer provides an output voltage proportional to this current. The device is available in a proprietary, 1 mm thick package that reduces eddy current losses to improve sensor output bandwidth when compared to more conventional IC packages. Allegro SIP-based current sensors have a typical output bandwidth as high as 120kHz and offer high resolution, high accuracy performance that allows for higher speed control of the PWM switches in an inverter system. Additionally, these SIP sensors offer a 3 µs output response time for IGBT overcurrent protection applications. The form factor of this solution is also much smaller than bulky current transformers. The Allegro SIP package easily provides the necessary galvanic isolation because the sensor output leads are not connected to the high voltage, current carrying conductor in each phase of the motor.

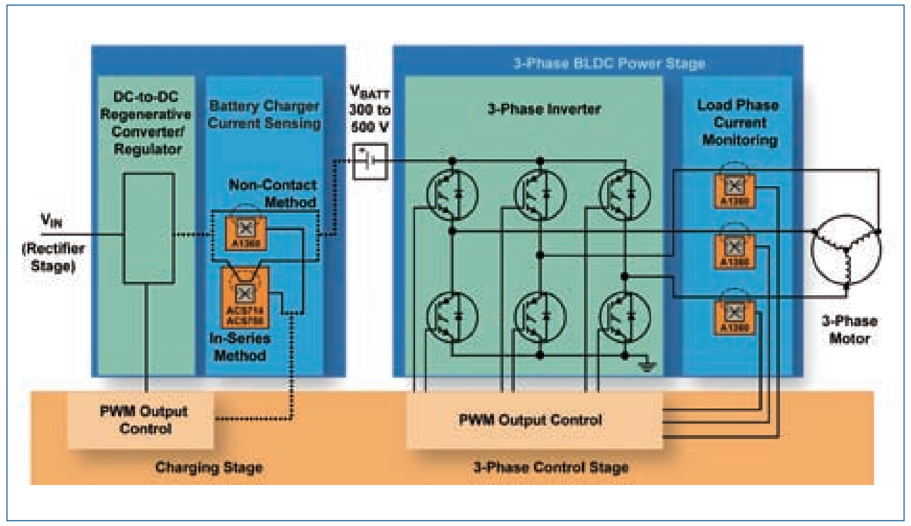

Figure 3a: DC-DC converter charger *Figure 3b: Three-phase DC-AC inverter*

DC-DC converters

The current sensing range and the isolation voltage required determine the optimum Allegro current sensor package for use in DC-DC converters.

Current sensors in DC-DC converters often need to sense current down to DC frequencies. This need precludes the use of current transformers in fully optimized systems. Using shunt resistors in these applications is also challenging (or impossible) since the high input or output DC voltages require expensive, high common-mode input operational amplifiers. As a result of the inherent galvanic isolation of Allegro Hall effect sensor ICs, and their ability to sense both DC current and high frequency current signals, they are a logical choice for HEV DC-DC converter applications.

A simplified regenerative DC-DC converter is shown in Figures 1 and 3a. The regenerative converter utilizes a current sensor that can operate at battery voltage levels. Accurately sensing the converter output current is a critical function as HEV battery life is extended by limiting the charge current delivered to the battery.

The ACS714 current sensor is ideal for many lower current, subsystem DC-DC converter applications and is a factory trimmed, galvanically isolated sensor that is available in an extremely small form factor SOIC8 package with an integrated 1.2mΩ conductor for low power loss. Additionally, the Allegro ACS758 device incorporates both a 100µΩ conductor and a ferromagnetic core into a small form factor, galvanically isolated package capable of sensing 50 through 200A. Currents above 200A can be sensed with the SIP based toroid configuration mentioned earlier. All of these Allegro solutions offer industry leading high bandwidth output performance and exceptional current resolution capabilities.

Summary

Allegro's latest generation Hall effect current sensor IC technology offers significant advantages in sensing both AC and DC currents in HEVs. Hall current sensors have inherent galvanic isolation for high side current sensing, and offer low power loss in high efficiency HEV applications. Recent improvements in Hall IC technology by Allegro have resulted in the development of industry leading high bandwidth, high resolution current sensor ICs that are ideally suited for use in HEV Inverter and DC-DC converter applications.

www.allegromicro.com

Drive with Infineon's EiceDRIVERs™

Gate drivers using CLT technology for automotive hybrid and electric vehicles

In order to fulfil increasingly stringent requirements to improve fuel economy and to reduce emissions, the automotive industry is looking for innovative solutions. In the future, e-Mobility is expected to play a major role in the overall reduction of CO_2 emissions.

By Laurent Beaurenaut, Senior Staff Application Engineer, Electric Drive Train Systems, Infineon Technologies AG, Germany

The mass production of this technology is highly depending on the introduction of cost effective and reliable power electronics. Infineon's product portfolio, scaling from bare dies and discrete ICs to power modules, is aimed at helping the development of optimized system solutions for hybrid and electric vehicles.

In order for the electric motor to provide directly or indirectly traction energy to the vehicle, an inverter is used to convert the high-voltage battery dc voltage into ac signals driving the motor. Typically, an inverter is made of a high power IGBT module controlled by a smart logic operating in the low voltage (typically 12V) battery domain. Between the microcontroller and the IGBT switch stands a gate driver whose main role is to control optimally and safely the switching behaviour of the IGBT transistor. Infineon's 1ED020I12FA, 1ED020I12FTA and 2ED020I12FA automotive gate drivers have been specifically designed for this purpose.

A step towards smarter and safer drivers

Figure 1: 1ED020I12FA IGBT driver IC in PG-DSO-20-55 package

The microcontroller and the high-power stage need to be electrically insulated. Infineon has developed the Coreless Transformer Technology (CLT), which enables galvanic insulation up to 6kV (according to EN50178). The main idea of the coreless transformer technology is to integrate the two coils of a transformer into an integrated circuit. Data transfer is enabled bi-directionally in an inductive way. CLT offers multiple advantages in comparison to other technologies. First, it does not show the degradation over life time which is typically seen with optocouplers. Secondly, with appropriate design and packaging measures, it shows high immunity to electro-magnetic interferences and transients. Finally, it can be easily implemented within standard chip production processes, which leads to a reduction of system costs in comparison for example to discrete approaches. Moreover, while a discrete transformer needs a core to direct the magnetic flux the coils in an IC can be placed close enough to save the core. Infineon EiceDRIVER™ automotive family are all based on the CLT technology.

The 1ED020I12FA (Figure 1) is an advanced IGBT gate driver. It can source or sink up to 2A which makes it suitable to drive directly smaller MOSFET and IGBT power modules (up to 100A typically). Control and safety relevant functions are included in order to increase the reliability of the whole system. The driver consists of two galvanic separated parts: the input chip can be directly connected to a standard 5V DSP or microcontroller with CMOS standard I/Os, the output chip being connected to the high voltage side. The rail-to-rail driver output enables the user to clamp easily the IGBTs gate voltage during short circuit conditions, while at the same time limiting the power losses in the device.

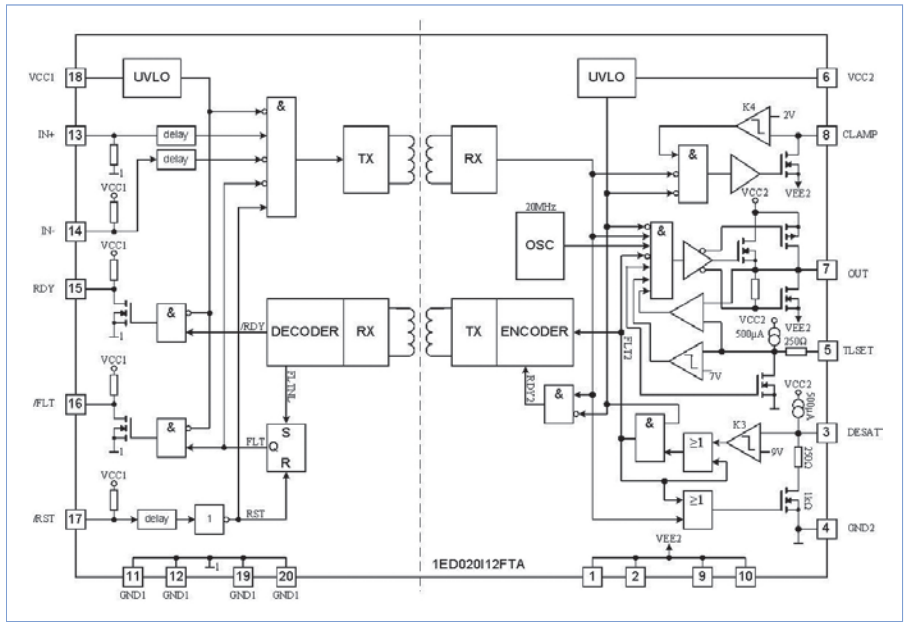

Figure 2: 1ED020I12FTA block diagram

The 1ED020I12FA has implemented several internal end external protection features. To ensure the correct switching of IGBTs, the device is equipped with separate under voltage lockout monitors for the primary and secondary sides. If the power supply voltage of either side drops below a given threshold, the IGBT is brought into a safe off-state. The PWM signals at the input are then ignored until the failing supply reaches a safe operating level again. In case of supply failure, a fast notification is sent to the microcontroller via the READY pin.

Internally, the integrity of the signal pace across the CLT is strengthened by several mechanisms. In order to limit the effect of single disturbances, the PWM signal commands (both ON and OFF) are resent at periodic intervals of about 500ns. A watchdog function is also used to monitor automatically the signal transmission across the CLT. If a failure is detected, the IGBT is switched off and the READY output reports an internal error to the microcontroller.

Externally, a desaturation protection (DESAT) ensures the protection of the IGBT in case of short circuit. The DESAT functionality monitors the voltage across the IGBT. When the voltage at the DESAT pin exceeds a threshold, the IGBT gate voltage is forced to low. Moreover, the FAULT output is activated, allowing a fast notification to the microcontroller. A programmable blanking time is used to suppress spikes and noise introduce by IGBT switching. Blanking time is controlled by a highly precise internal current source and an external capacitor.

The internal active Miller clamp function prevents the occurrence of parasitic turn-on effects during high dV/dt situations (for example when the other transistor of the leg switches on). During turn off, the gate voltage is monitored and the clamp output is activated automatically in order to provide a low impedance path to the parasitic current flowing through the Miller capacitance.

The 1ED020I12FTA is a further evolution as it provides an additional functionality: the Two Level Turn-Off (Figure 2). With this feature, the gate driver switches the IGBT off using two steps, i.e. by forcing the gate voltage to an intermediate value. Both plateau value and hold time are configurable. This way, too fast current variations can be avoided and therefore the collector-emitter voltage of the IGBT can be kept below the allowed maximum value.

The 2ED020I12FA goes one step further towards function integration since it provides high and low side isolated referenced outputs. The device consists of two galvanic separated drivers. The device also includes a DESAT protection with a FAULT status output for each of the drivers. Two READY status outputs reports if the device is supplied and operates correctly.

Samples of the 1ED020I12FA and 1ED020I12FTA can be order in PG-DSO-20-55 Package. Samples of the 2ED020I12FA in PG-DSO-36/32-1 Package will be available in September 2010.

Outlook

Over years, the general trend for electronic automotive systems has always been to go for more integration: the exponential increase of computational power of microcontrollers leads to the progressive replacement of hardware functions into software; digitalization leads to the introduction of smart sensors with enhanced functional and diagnostic capability. This general trend is also expected for the drivers, which are mainly relying today on analog technology. The realization of smart and cost-effective drivers, integrating a high share of digitalized functions and meeting functional safety requirements as per SIL and ASIL levels, will be one of the most exciting challenges the high-power automotive electronic manufacturers will have to face in the coming years.

www.infineon.com

Next Generation Automotive

Compact and efficient power electronics enablers

With the recent upsurge in hybrid vehicle adoption and almost all major car OEMs now working on full electric vehicle projects, people often point out that this is old news. In many respects they are correct; the origins of the electric car can be traced back to the 1830s and by the late 1890s fleets of electric taxi cabs were running around the streets of several US cities. So what's different this time round?

By Benjamin Jackson, Product Manager, Automotive MOSFETs, International Rectifier

There have been two major barriers to the electrification of the car to date. The first is the dominance of the existing technology. In short the internal combustion engine is just too good. Modern engines are mass produced, cost effective, well understood, highly refined & reliable and supported by a universally established refueling and repair infrastructure. Now as governments scrutinize CO_2 emissions, the internal combustion engine is coming under pressure from both ends with heavy taxes on the gasoline put into the tank and on the emissions flowing out of the exhaust. The second major obstacle to the electrification of the car is energy density. The main enablers here will be new battery technology and novel battery management schemes. But at the same time the systems which use the limited onboard supply of electrical energy will have to do so in a more intelligent way. An increasing awareness of efficiency is fueling a rapid change in the application landscape across all vehicle types. High power DC-DC converts, HID lighting, class D audio, electric power steering, 3 phase inverters and synchronous rectification will appear in increasing numbers on next generation cars, offering efficiency and good power density. Power MOSFETs will be a key enabling technology in both controlling the battery and its loads.

By their nature power MOSFETs are not 'ideal' switches. MOSFETs have a finite on-resistance, add parasitic parameters to the electrical path and, the more power needed the more space is required for switches and cooling assemblies. These all affect the power density and efficiency of a given power electronics system. How can this be improved?

The power dissipation in the steady state of a semiconductor can be expressed as:

$$Pd = \frac{T_j - T_A}{R_{thJA}}$$

(1) Where Pd is the power dissipated in the semiconductor switch, T_j is the junction temperature, T_A the ambient temperature of the surroundings and R_{thJA} is the total thermal resistance from junction to ambient.

Also considering the relationship between power, current and $R_{DS(on)}$

$$P_d = I_D^{\,2} R_{DS(on)}$$

(2) Combining 1 and 2 together we can link the current to the thermal resistances and the $R_{DS(on)}$:

$$I_D = \sqrt{\left(\frac{T_j - T_A}{R_{thJA}}\right) / R_{DS(on)}}$$

(3) This equation is important as it shows how the thermal management aspects of the design have a direct impact on the electrical performance of the system.

Finally dividing by the area of the MOSFET's PCB footprint, A_{FP}, we can arrive at the current density of the device:

$$CurrentDensity = \frac{\sqrt{\left(\frac{T_j - T_A}{R_{thJA}}\right) / R_{DS(on)}}}{A_{FP}}$$

(4) On closer inspection of equation 4 the main obstacles to greater current density can seen.

Minimize thermal resistance → Maximize heat extraction

The first step to increasing power density is to ensure that for a given $R_{DS(on)}$ the silicon in housed in a package which enables the heat generated to be easily extracted; R_{thJA} must be as low as possible.

To keep R_{thJA} low semiconductor designers can increase the size of the silicon die, getting more die in contact with the package enables a better heat transfer to the outside world, a larger die archives this and has lower $R_{DS(on)}$, but at greatly increased cost. Alternatively the thermal resistances of the package can be reduced, perhaps with new materials or a new style of package. Most traditional power packages only have a single cooling path; through the bottom of the device to the PCB or heat sink. Great improvements can be made with the addition of a secondary cooling path; this is exactly what the DirectFET package enables via top side cooling.

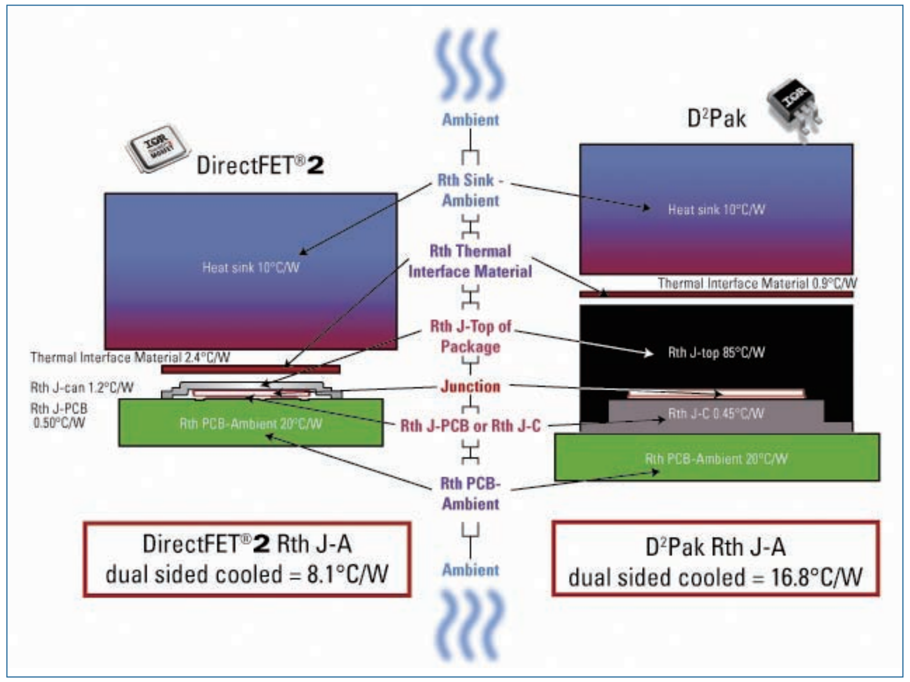

Figure 1: Comparison of cooling routes for a D2Pak and large can DirectFET package

Figure 1 compares and contrasts the thermal routes for getting the heat out of a Large Can DirectFET package and a D2Pak. In both cases the designer has attempted to achieve the lowest possible thermal resistance from junction to ambient by using both the downward thermal path from the junction to the PCB and the upward path through the package to a heat sink on top of the part.

Both packages have good thermal resistance from the junction to the PCB with values of 0.5°C/W and 0.45 °C/W for the $R_{th\ J\text{-}PCB}$ of the DiretcFET and D2Pak respectively. By adding a second upwards thermal path these values can be reduced. The D2pak was not designed to be cooled through the top of its thick plastic package, but if this is attempted an $R_{th\ J\text{-}TOP}$ (junction to top of package thermal resistance) of around 85°C/W will be seen compared to the DirectFET which has an considerably lower value of 1.2°C/W. When the overall thermal resistances of the two routes in parallel are compared the dual sided cooled DirectFET has a thermal resistance which is around half of the D2Pak. Using the second thermal route enables an instant improvement in the current density of the system.

Keep $R_{DS(on)}$ low

Looking at the numerator of equation 4 after having kept R_{thJA} low it's then important to consider the root cause of the heating – the on resistance of the device. A key figure of merit here is the semiconductor material and the design of the MOSFET itself. However silicon based MOSFET technology is maturing forcing manufacturers have to look to further afield to complex silicon solutions or new materials to keep the $R_{DS(on)}$ low. But it is also important to consider the effect of the package on the $R_{DS(on)}$ value or rather the limitations that the package places on delivering ultra low $R_{DS(on)}$ to the system.

MOSFETs with an on resistance in the 1mΩ range at 40V are reasonably common in the market today and increas-

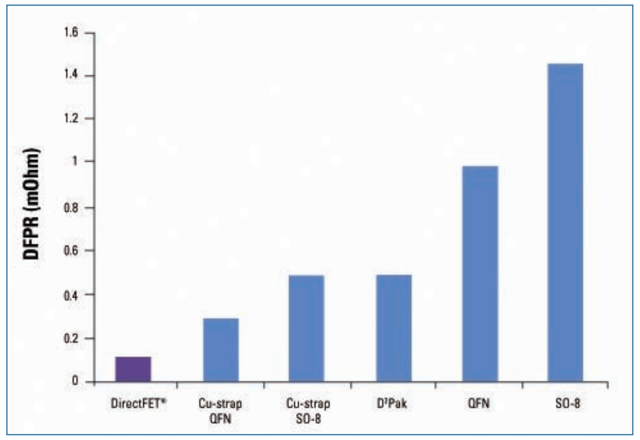

Figure 2: Comparison of die free package resistances for different power packages

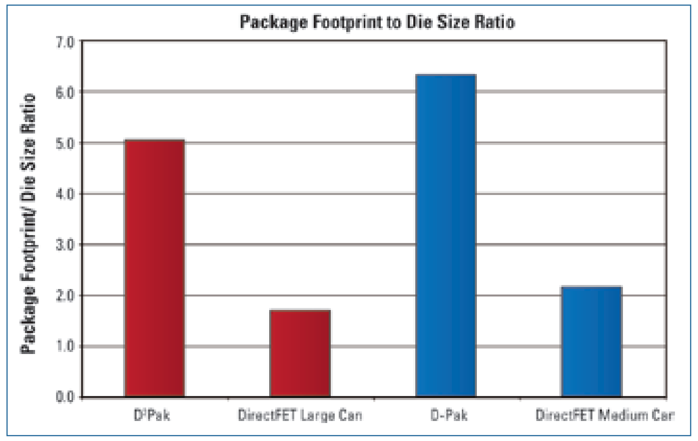

Figure 3: Package footprint to maximum die size area ratio for different power packages

Part	AUIRFS3004-7P	AUIRF7739L2
Package	D2Pak-7P	Large Can DirectFET
PCB Footprint	170 mm²	64 mm²
Single Side Cooled on FR4		
R_{thJA} (Single side cooling)	40 ° C/W	40 ° C/W
$R_{DS(on)}$ @ T_j = 105° C, T_A = 25 ° C	1.24 mΩ	0.9 mΩ
I_D	40.1 A	46.3 A
Current Density	0.24 A/mm²	0.73 A/mm²
Ratio of current density	**1**	**3.1**
Dual Sided Cooled		
R_{thJA} (Dual side cooling DF only)	40 ° C/W	12.5 ° C/W
$R_{DS(on)}$ @ T_j = 105° C, T_A = 25 ° C	1.24 mΩ	0.9 mΩ
I_D	40.1 A	82.8 A
Current Density	0.24 A/mm²	1.30 A/mm²
Ratio of current density	**1**	**5.5**

Table 1: Comparison of current density for a D2Pak-7P and a large can DirectFET with different cooling arrangements

ingly on such devices around half of the $R_{DS(on)}$ stated on the datasheet is attributed to the package. The resistance that the package adds to the silicon is know as the Die Free Package Resistance (DFPR) and figure 2 shows the DFPR values for various power packages.

There is a large range in DFPR values between the existing plastic packages (shaded in green). Different wire bonding and lead frame options enable the DFPR to be greatly reduced to around 0.3mΩ in the case of the copper clip PQFN. However the lead frame and wire bonds on the traditional plastic packages still leave a relatively long electrical path between PCB and die. As the market continues to demand more efficient systems, at higher power levels, $R_{DS(on)}$ values will hit a fundamental limit at the resistivity of the conductors in the packaging. When the wire bonds and leadframe removed (in the case of DirectFET) the DFPR is reduced to a value of less than half of best performing equivalent plastic power package at a mere 150μΩ. This enables very low $R_{DS(on)}$ and the best possible current density for a given semiconductor technology. Furthermore the dramatic reduction of the DFPR barrier ultimately means that a lower area of silicon is needed to deliver a given $R_{DS(on)}$ to the system and thereby opening up the possibility of cost savings.

Go small to be effective

Finally turning to the denominator of equation 4 it's clear and logical that ultimately the smaller the footprint of the MOSFET greater the current density. But such a reduction in package footprint area must not be done at the expense of $R_{DS(on)}$ or current rating. Ideally the designer wants to get the lowest $R_{DS(on)}$ possible in a given space. As die size and $R_{DS(on)}$ are inversely proportional, calculating the ratio of package footprint area to maximum die size area for the given package is an indication of the $R_{DS(on)}$ performance that a given package can offer in a given space. Figure 3 plots the ratio of package footprint to maximum die size area.

In figure 3, the ideal ratio would tend towards 1, giving the least mm2 of PCB footprint to achieve a given $R_{DS(on)}$. However figure 3 clearly shows the area overhead that the more traditional packages such as the DPak and D2Pak place on the die size area, and ultimately the reduction in current density. The D2Pak has a package footprint to maximum die size area ratio of 5; the package area is five times the size of the largest die size. The Large Can DirectFET however offers a ratio of around 1.7 – so ultimately on the PCB you can achieve a given $R_{DS(on)}$ in a smaller space and therefore at a higher current density as well as saving on PCB and enclosure space.

Drawing the factors of space, $R_{DS(on)}$ and R_{thJA} together, table 1 (using equation 4) makes a side by side comparison of a low $R_{DS(on)}$ D2pak product with a counterpart Automotive DirectFET product. The table summarizes the improvement in current density.

By taking two high performance 40V power MOSFETs which are typically used in automotive applications table 1 shows how current density can be improved by over 3 times due to the low package resistance and small PCB footprint of the DirectFET package. When dual sided cooling is employed the DirectFET can further improve its margin to over 5 times the current density of the D2Pak.

The adoption of new fuel efficient vehicles has been kick-started by financial, environmental and political forces of the last few years. But the electrification of the car will only be a long term success if new electrical solutions prove they can overcome the technical and practical dominance of the existing internal combustion engine and its drive train. This has proven to be too greater hurdle over the last 170 years, but today, with highly efficient, cost effective & compact power semiconductors and battery technology the links to the successful electrification of the car are beginning to connect. The humble package which holds the small and delicate semiconductor it important to protect the device from its environment but it also serves an important role as the performance gatekeeper between the die and the PCB. As tougher performance goals are set bringing the packaging technology of power semiconductors up to date will be key to unlock the maximum performance from existing silicon MOSFETs and the next generation compound semiconductors.

www.irf.com

Essential Multicell Monitoring

Maximizing the cycle life of rechargeable battery packs

Rechargeable battery packs prematurely deteriorate in performance if any cells are allowed to over-discharge, for example, in hybrid automobiles or lower-cost products like portable tools and backup power sources. As a pack becomes fully discharged, the ILOAD • RINTERNAL voltage drop of the weakest cell(s) can overtake the internal VCELL chemical potential and the cell terminal voltage becomes negative with respect to the normal voltage

By Jon Munson, Senior Applications Engineer, Linear Technology Corporation

In such a condition, irreversible chemical processes begin altering the internal material characteristics that originally provided the charge storage capability of the cell, so subsequent charge cycles of the cell do not retain the original energy content. Furthermore, once a cell is impaired, it is more likely to suffer reversals in subsequent usage, exacerbating the problem and rapidly shortening the useful cycle life of the pack.

With nickel-based chemistries, an over-discharge of a set of series-connected cells does not necessarily lead to a safety hazard, but it is not uncommon for one or more cells to suffer a reversal well before the user is aware of any significant degradation in performance. By then, it is too late to rehabilitate the pack. In the case of the more energetic lithium-based cell chemistries, reversals must be prevented as a safety measure against overheating or fire. Monitoring the individual cell voltages is therefore essential to ensure a long pack life (and safety with lithium cells).

Enter the LTC6801, developed to provide integrated solutions for these specific problems. The LTC6801 can detect individual cell overvoltage (OV) and undervoltage (UV) conditions of up to twelve series connected cells, with cascadable interconnections to handle extended chains of devices, all independent of any microprocessor support.

Features of the LTC6801

The operating modes and programmable threshold levels are set by pin-strap connections. Nine UV settings (from 0.77V to 2.88V) and nine OV settings (from 3.7V to 4.5V) are available. The number of monitored cells can be set from 4 to 12 and the sampling rate can be set to one of three different speeds to optimize the power consumption versus detection time. Three different hysteresis settings are also available to tailor behavior of the alarm recovery.

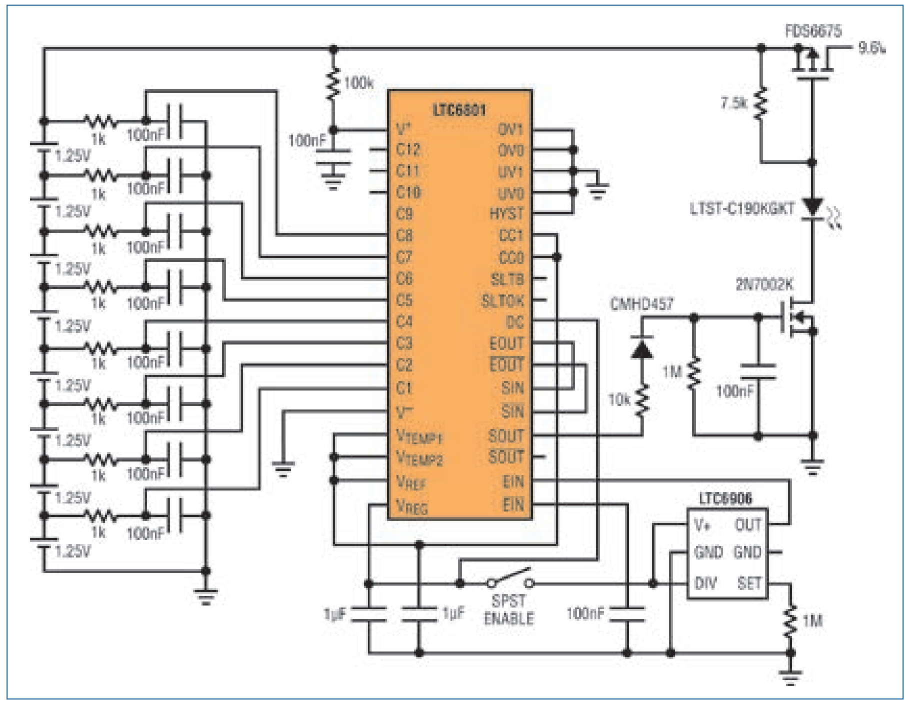

Figure 1: An 8-cell nickel pack can be easily monitored and protected from the abuse of over-discharge

Special Report – Automotive Electronics

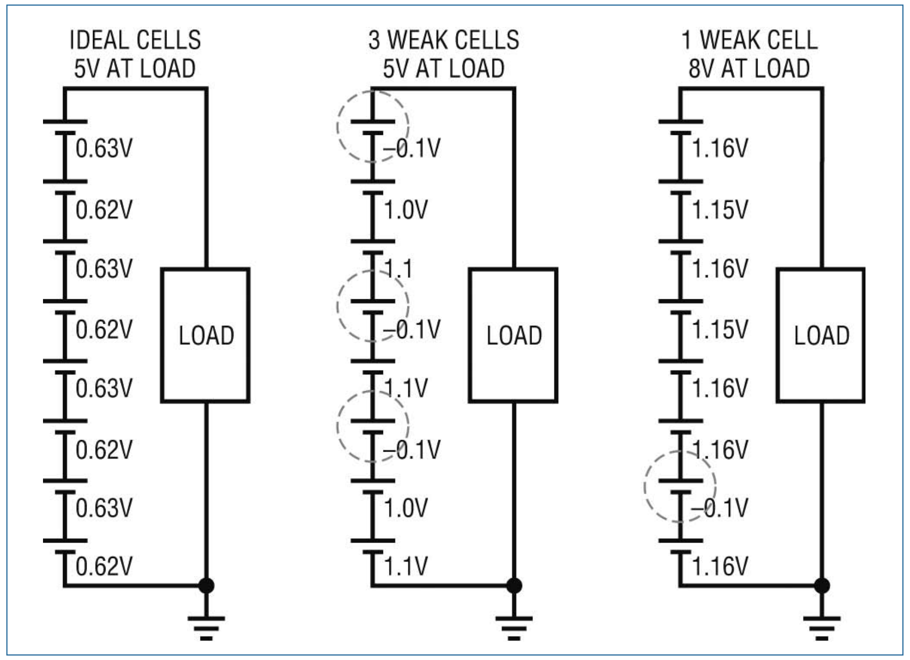

Figure 2: Real-world cell performance

To support extended configurations of series-connected cells, fault signaling is transmitted by passing galvanically isolated differential clock signals in both directions in a chain of "stacked" devices, providing excellent immunity to load noise impressed on the battery pack. Any device in the chain detecting a fault stops its output clock signal, thus any fault indication in the entire chain propagates to the "bottom" device in the stack. The clock signal originates at the bottom of the stack by a dedicated IC, such as the LTC6906, or a host microprocessor if one is involved, and loops completely through the chain when conditions are normal.

In many applications, the LTC6801 is used as a redundant monitor to a more sophisticated acquisition system such as the LTC6802 (for example, in hybrid automobiles), but it is also ideal as a standalone solution for lower-cost products like portable tools and backup power sources. Since the LTC6801 takes its operating power directly from the batteries that it monitors, the range of usable cells per device varies by chemistry in order to provide the needed voltage to run the part— from about 10V up to over 50V. This range supports groupings of 4–12 Li-ion cells or 8–12 nickel-based cells. Figure 1 shows how simply an 8-cell nickel pack can be monitored and protected from the abuse of over-discharge. Note that only an undervoltage alarm is relevant with the nickel chemistries, though a pack continuity fault would still be detected during charging by the presence of an OV condition.

Avoiding Cell Reversals

Cell reversal is a primary damage mechanism in traditional nickel-based multicell packs and can actually occur well before other noticeable charge-exhaustion symptoms set in.

Consider the following scenario. An 8-cell nickel-cadmium (NiCd) pack is powering a hand tool such as a drill. The typical user runs the drill until it slows to perhaps 50% of its original speed, which means that the nominal 9.6V pack is loading down to about 5V. Assuming the cells are perfectly matched as in the left diagram of Figure 2, this means that each cell has run down to about 0.6V, which is acceptable for the cells. However, if there is a mismatch in the cells such that perhaps five of the cells are still above 1.0V, then the other three would be below zero volts and suffer a reverse stress as shown in the middle diagram of Figure 2.

Even assuming that there is only one weak cell in the pack (a realistic scenario) as in the right diagram in Figure 2, the first cell reversal might well occur while the stack voltage is still 8V or more, with just a subtle reduction in perceived pack strength. Because of the inevitable mismatching that exists in practice, users unknowingly reverse cells on a regular basis, reducing the capacity and longevity of their battery packs, so a circuit that makes an early detection of individual cell exhaustion offers significant added value to the user.

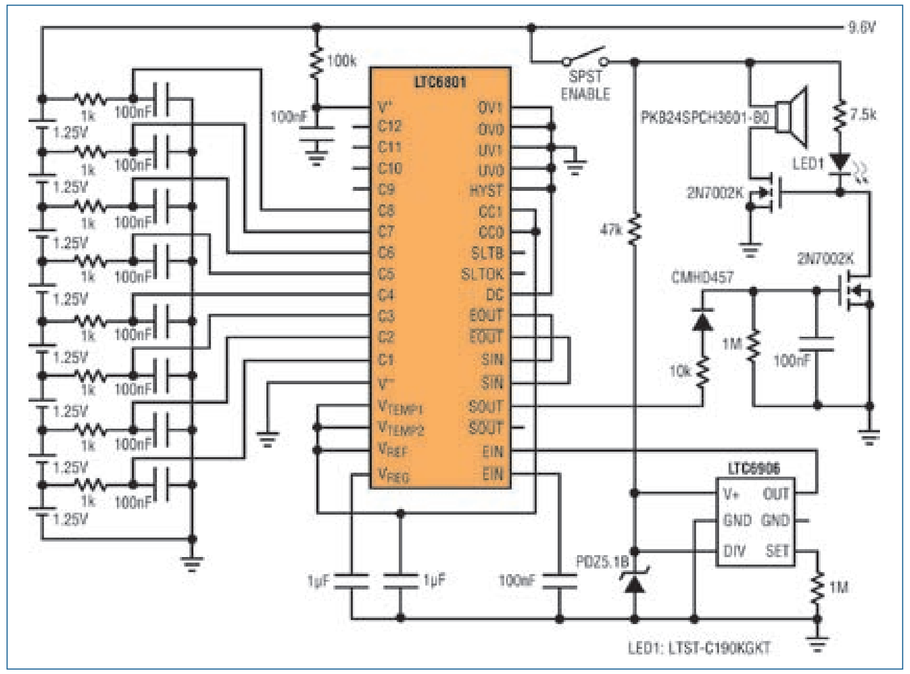

Figure 3: Circuit to provide an audible alarm indication that the battery is near depletion

Using the LTC6801 Solution

The lowest available UV setting of the LTC6801 (0.77V) is ideal for detecting depletion of a nickel-cell pack. Figure 1 shows a MOSFET switch used as a load disconnect, controlled by the output state of the LTC6801. Whenever a cell becomes exhausted and its potential falls below the threshold, the load is removed so that cell reversal and its degradation effects are avoided. It also allows the maximum safe extraction of energy from the pack since there are no assumptions made as to the relative matching of the cells as might be the case with an overly conservative single pack-potential threshold function.

A 10kHz clock is generated by the LTC6906 silicon oscillator and the LTC6801 output status signal is detected and used to control the load disconnect action. Since this example does not involve stacking of devices, the cascadable clock signals are simply looped-back rather than passed to another LTC6801. An LED provides a visual indication that power is available to the load. Once the switch opens, the voltage of the weak cell tends to recover somewhat and the LTC6801 reactivates the load switch (no hysteresis with 0.77V undervoltage setting). The cycling rate of this digital load-limiting action depends on the configuration of the DC pin; in the fastest response mode (DC = V_{REG}), the duty cycle of the delivered load power drops and tapers off, with pulsing becoming noticeable and slower as the weakest cell safely reaches a complete discharge.

In some applications it is not acceptable to spontaneously interrupt the load when the weakest cell is nearing full discharge as depicted in Figure 1. For those situations, the circuit of Figure 3 might be a good alternative. This circuit does not force a load intervention, but simply provides an audible alarm indication that the battery is near depletion. Here the LED provides an indication that the alarm is active and that no cells are exhausted.

An LTC6801 idle mode is invoked whenever the source clock is absent, and power consumption then drops to a miniscule 30μA, far less than the typical self-discharge of the pack. In both figures, the circuits show a switch that disables the oscillator (and other peripheral circuitry) in order to place the circuit into idle mode when not being used so that battery drain is minimized.

Conclusion

The LTC6801 simultaneously monitors up to 12 individual cells in a multicell battery pack, making it possible to maximize the pack's capacity and longevity. It can also be cascaded to support larger battery stacks. The device has a high level of integration, configurability and well thought out features, including an idle mode to minimize drain on the pack during periods of inactivity. This makes the LTC6801 a compact solution for improving the performance and reliability of battery powered products.

www.linear.com

Swifter, Higher, Stronger –

The Olympic generation of automotive video interfaces

According to IMS Research the number of video capable automotive head units will grow from 8.5 Mu in 2006 to 26.6 Mu in 2015. In order to present the information to the driver with less distraction from car traffic, the displays will need to be installed in places which are remote from the actual head unit, e.g. in the top area of the middle console, the instrument cluster or as head up displays, projecting to the back of the windscreen.

By Dr. Thomas Wirschem, Product Marketing Manager, High-Speed Data Division Europe, National Semiconductor

The video interfaces, tying graphics sources and panels together, are more and more converting from analog video technology to the higher quality RGB (Red Green Blue) digital video format which is the standard interface used within LCD displays. While for the front display applications cable lengths typically stay in the range of 1-3 meters, the Rear Seat Entertainment (RSE) units on the other hand can require cable reach of 8 meters and beyond. Such connections supporting data rates in the Gigabit/sec region, far beyond the baud rates of conventional automotive board networks, can nicely be addressed with point-to-point Serializer/Deserializer (SerDes) solutions. Such chipsets greatly reduce the number of transfer wires and connector pins in comparison to transporting a wide, parallel video bus thus offering tremendous system-level advantages. The DS90UR905/6 and DS90UR907/8 SerDes chipsets have been developed by National Semiconductor to address the especially harsh requirements for automotive display interfaces in terms of high data throughput, ultrathin cabling, advanced signal conditioning, testability and ultra-low EMI (Electro Magnetic Interference). They represent the industry' s first embedded clock SerDes solutions to span resolutions from Quarter Wide VGA (400 x 240) and up to XGA (1024 x 768) at 24-bit color depth. This wide range of pixel clock frequencies allows the car manufacturers to employ just one digital video display interface solution throughout their portfolio of car models from small instrument cluster panels over dual view, center stack LCDs to larger format RSE displays.

Video applications and SerDes concept

The targeted application for the SerDes components is a Flat Panel Display Link interface connecting a graphic host to a display over a long serial cable. Typical examples range from Central Information Displays (CID) to instrument cluster panels to entertainment LCDs in the headrest or flip-down modules from the roof for rear seat passengers as shown in Figure 1.

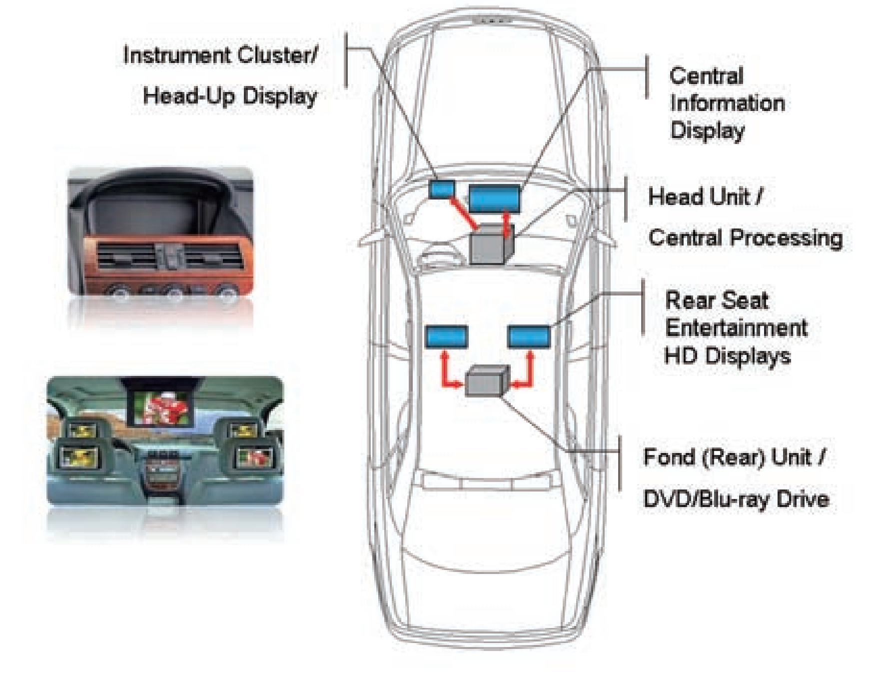

Figure 1: Examples of remoted automotive display applications

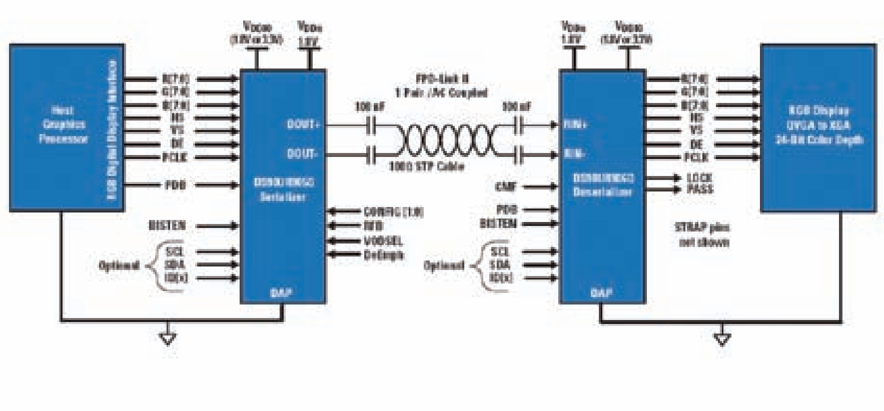

Figure 2: Video transfer with the DS90UR905/6 SerDes chipset

These new chipsets are part of the "FPD-Link II" product family of National Semiconductor and translate 27 bits of digital RGB color and timing control signals from a video source into one single, serial data stream with embedded clock information over a twisted pair of wires. This video transfer concept is depicted in Figure 2 on a system level.

The chipsets can support either 18-bpp (bits per pixel) or 24-bpp color depth applications. The pixel clock range has been designed to be extremely wide from 5MHz up to 65MHz frequency. This translates in serial line rates from 140Mbps (bits per second) to 1.82Gbps, covering all mainstream resolutions of automotive displays. The SerDes chipsets require NO external reference clock (quartz or oscillator) to "pre-synchronize" the receiver's PLL within a certain frequency band around the transmitter's parallel clock. The DS90UR907/8 chipset has the same features as the DS90UR905/6 chipset with the difference that the inputs and outputs are no longer parallel busses with LVCMOS signaling, but still comply with the open-industry "FPD-Link" standard. Many state-of-the-art graphic controllers, display timing controllers, ASICs and FPGAs support this "first level of serialization" which employs either 3 data lanes for 18bpp or 4 data lanes for 24bpp, each with a parallel clock channel. The electrical signaling is according to the open ANSI/TIA/EIA-644A standard, also known as "LVDS" (Low Voltage Differential Signaling). The advantages of using this interface option instead of the conventional LVCMOS are lower EMI levels through differential signaling and reduction of component pin count, as illustrated in Figure 3.

Power over FPD-Link

Both display and camera applications can greatly benefit from having the power transferred from their respective link partners over the video data cable. In the case of a navigation panel the power could be sourced from the head unit and in the case of a camera imager the power could come from its respective electronic control unit. The main advantage of such concepts is the significant reduction of the overall cable harness and board connectors. This can lower cabling cost and weight, while enabling the smaller footprint designs that can be essential for tiny imager modules used, for instance, in outside mirror locations.

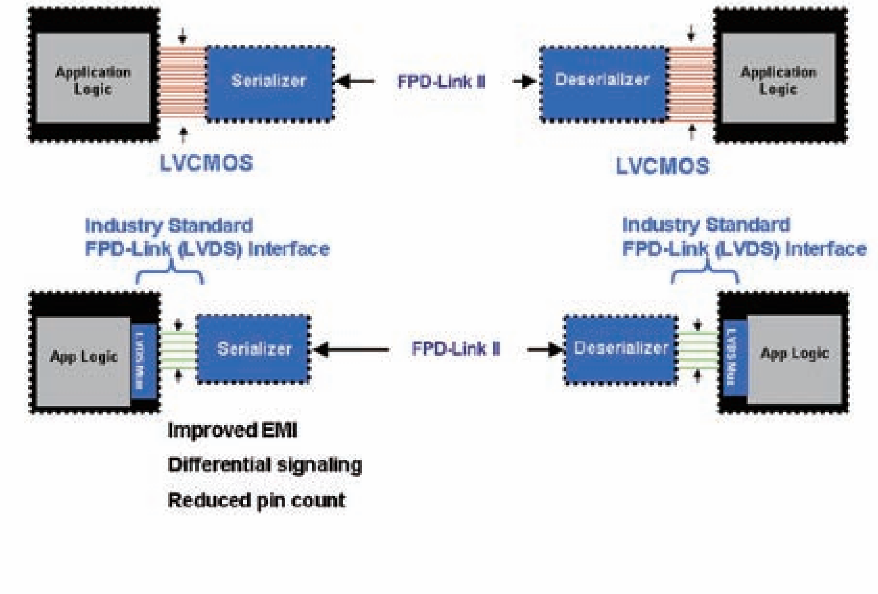

Figure 3: Advantages of "FPD-Link" system interface option

Figure 4 shows a block diagram on how power can even be inserted and extracted on the very same pair of wires, that National Semiconductor FPD-Link II and FPD-Link III chipsets are using for video, audio and data transfer. Hence this approach is called "Power over FPD-Link". This topology is needed for a solid powered data line. A Bias-T filtering is recommended for a close to noiseless power insertion, which isolates the high-speed data from the power line. A ground isolation topology (with isolated flyback) avoids the return current through the boost converter path. The overall performance depends of course strongly on the system ground and shielding concepts. In practical setups power ratings of over 25 Watts could be achieved at the remote link partner, when working with insert voltages of 12-14 Volts (from car battery). This easily accommodates the power consumption of driver assistance camera modules (1-3 Watts) and most

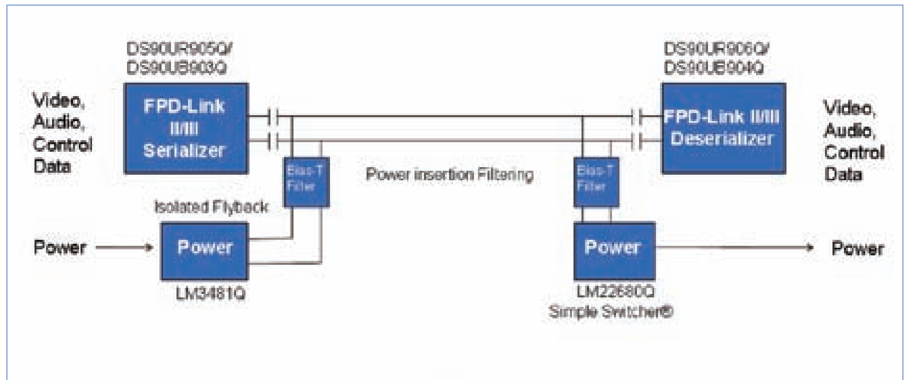

Figure 4: Power over FPD-Link – basic block diagram

standard infotainment displays (15-20 Watts).

Chipset enhancements

The deserializer is enhanced with an integrated, configurable Spread-Spectrum Clock (SSC) generator. At the receiver output bus this leads to a slight variation of the output clock frequency and data spectrum over time at very low modulation rate of a couple ten kiloHertz. As described in Figure 5, the frequency variation can happen around the nominal pixel clock center frequency ("center spread modulation") or towards lower frequencies ("down spread modulation"). The spreading of the spectrum can be as high as plus or minus 2%. Instead of switching all outputs at the same point in time and at a constant frequency while exhibiting a narrow band of radiation noise, the Spread-Spectrum Clocking is distributing the peak energy over a wider spectral range, thus reducing the EMI noise level significantly. With all output data synchronized to the output clock, both data and clock are effectively spread. Particularly with the Low Voltage (LV) CMOS interface option at the DS90UR906 receiver output, this feature can drastically reduce electromagnetic radiation. Further enhancements include the integrated termination resistors, which reduce the complexity of the board design and lead to lower cost and less board space. The chipset supports a very wide temperature range of -40°C to +105°C. This opens application areas in a variety of automotive electronics systems where displays

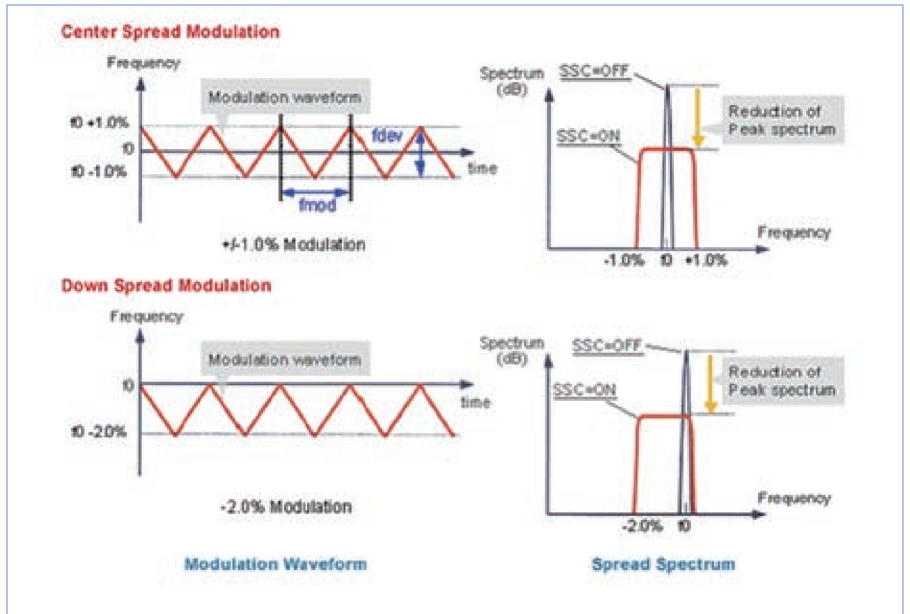

Figure 5: Spread-Spectrum Clocking (SSC) lowers harmonic peaks

need to be exposed to very high or very low temperature environments. The chipsets are offered in small footprint, Leadless Leadframe Package (LLP) options at a mere 1mm thickness, which are of course lead free and RoHS compliant. This industry standard packaging type exhibits outstanding electrical and thermal characteristics and is well suited for standard manufacturing handling and inspection. Not at last the chipsets are fully automotive qualified according to AEC-Q100 Grade 2 standard.

Summary

The new DS90UR905/6 and DS90UR907/8 FPD-Link II chipsets deliver many strong system benefits and enhancements. The parallel video bus is serialized into a single pair with an embedded clock. This lowers system cost, eliminates clock/data skew issues, reduces noise, and extends the link to long cable distances. The chipsets support all common automotive LCD resolutions from QWVGA to XGA at 24-bit color depth. Special attention has been paid to EMI mitigation features in order to facilitate system design, qualification and approval. Consequently this minimizes expensive shielding requirements, while not sacrificing robustness. The FPD-Link II chipset family represents an automotive optimized, true plug 'n' play solution due to its no compromise combination of low wire count, high bandwidth, low power, low EMI, ruggedness and autonomous link synchronization. Not at last it has been demonstrated that power transfer concepts can use the same pair of wires without disturbing the video link, enabling lighter, cheaper cable assemblies and less, smaller form factor board connectors to be used.

References

DS90UR905/6 Product folder:
http://www.national.com/mpf/DS/DS90UR905Q.html

DS90UR907/8 Product folder:
http://www.national.com/pf/DS/DS90UR907Q.html

LVDS Owner's Manual:
http://www.national.com/analog/interface/lvds_owners_manual

www.national.com

Automotive Air-Con Made Easy

Automatic HVAC air recirculation with stepper motors

In most automotive HVAC systems, a continuous inflow of fresh air is conditioned and brought into the cabin. Typically the driver can select whether the fresh air supply needs to be interrupted (recirculation) or not (fresh air open). In recirculation mode, high-end HVAC systems monitor several cabin air parameters, recirculate the air through the air conditioning unit back into the cabin and limit the fresh air inlet to the minimum, while fulfilling the air parameters set by the driver and/or the system's specifications. Such automatic recirculation can reduce the fuel consumption of an HVAC system by 35%.

By Bart De Cock and Steven De Preter, ON Semiconductor, Belgium

Depending on the climatic conditions and driving cycles, an HVAC system can consume up to three litres of fuel per 100km. This indicates that large cars that are equipped with a low-end HVAC system will benefit the most from the addition of an automatic recirculation function. However, small- and medium-sized cars that have advanced engines with low emissions will also benefit from a smart air-recirculation flap because the contribution of the HVAC fuel consumption is relatively high.

Forecasts indicate that the percentage of cars equipped with a semi- or fully-automatic HVAC system will increase year-on-year. At the same time, the introduction of CO_2 refrigerants leads to the potential requirement for additional sensors to be mounted in the cabin. These trends mean that the CO_2 and other fresh-air sensor technologies already available will increasingly be re-used in small cars and/or in cars with low-specification HVAC systems.

While the sensor aspect of the automatic recirculation function may have been solved, there is still some work needed to tackle the issues around flap motorization

.

Automatic Air Recirculation Control System

The HVAC Electronic Control Unit (ECU) closes the control loop of the fresh air regulation and operates the recirculation flap actuator (Figure 1) in order to maintain the required CO2 levels in the cabin. The frequency of operation of the circulation flap is a function of the maximum allowed number of occupants, the minimum volume of air in the car interior and the maximum allowed deviation from the desired CO_2 level. It is easily calculated that five people in a 3m3 interior will increase the CO2 concentration by 100ppm within 30s.

The air recirculation control loop requires mainly low-speed interventions to compensate for pressure and airspeed changes in the "Fresh Air Inlet" (Figure 1). This happens frequently when the driving speed varies, for example in - or in the vicinity of - cities. The airflow also changes with automatic blower speed adjustments to cancel fluctuations in sun radiation (e.g. due to a winding road or intermittent shade caused by buildings, trees or clouds).

The air recirculation flap actuator is a small motorized valve that is operated by means of a driver inside the ECU. For stable control algorithms, the flap position should be known at all times, so some sort of position feedback is a must. Because the control system is frequently re-adjusting the actuator position, contact-less operation of the motor and senseless position feedback is desired.

Recirculation Flap Technologies

Several solutions exist to move HVAC air flaps, including the recirculation air flap. They differ in type of motor used in the flap actuator and the specifics and features of the motor control. We will now discuss three

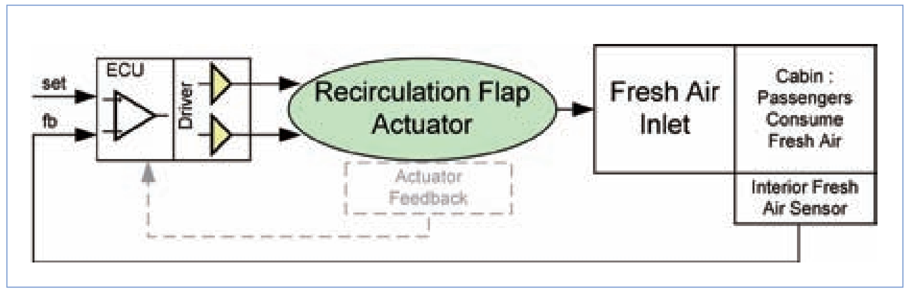

Figure 1: Automatic recirculation system

commonly used motor types.

Brushed DC (BDC) motors are made in a mature and relatively inexpensive technology. Only two wires lead from the driver to the motor terminals. It is simple to control a BDC motor; e.g. bidirectional drive can be achieved by means of two transistor half-bridges. In case position feedback is required – as with the air recirculation flap - a position sensor needs to be added. A variety of sensors exist, the most common being potentiometers. This sensor together with the associated ECU wiring and the impact of the size of the electrical connector makes up a significant part of the system cost. It is also important to note that the brushes and commutator are the parts of a BDC motor that are most prone to wear. Because of the need for frequent operation of the air recirculation flap, brush degradation puts a stress condition on the long-term mechanical reliability of a recirculation flap equipped with a BDC motor.

A unipolar stepper motor has two windings per phase. These windings are electrically connected with the ECU and, as with the BDC motor solution (with sensor position feedback), typically requires five wires. The choice of using unipolar stepper motors in motorized valves has mainly been dictated by the availability of low-cost driver ICs or driver circuits; e.g. a 4 low-side driver circuit. One drawback of the unipolar approach is that only half the number of windings is energized at any time (basically the unipolar stepper motor carries double the amount of copper than that required to move the motor).

A bipolar stepper motor has one winding per phase. Compared to a unipolar motor, this gives a size and weight advantage because the amount of copper in the winding is roughly half of that for a bipolar motor with similar motor characteristics. The two windings are electrically connected with the ECU by means of only four wires (compared to five wires for a unipolar stepper motor or a BDC motor with sensor). A bipolar stepper motor is typically driven by a dual full-bridge transistor combination, one for each winding. Compared to BDC and unipolar stepper architectures, new bipolar stepper motor actuator technologies offer a balanced solution: more system benefits (i.e. an optimized mix of features and quality) without overall system cost penalties. The main reason for this is that bipolar stepper motors inherently contain a "virtual" sensor and the motor's operation modes (running at speed, stall condition, etc) can be deducted from monitoring the back-electro-mechanical force or the bemf signal.

Virtual Sensor Benefits

An embedded stall detection algorithm based on the bemf signal, allows the system to detect very accurately the end-stop of a flap. Typically this end-stop is reached on purpose during a movement – for example when the flap is operated in a near-closed position. The closed-loop aspect (or merely pseudo closed-loop) consists of running deliberately into stalled condition once in a while. The stall detection then allows accurate marking of the new positions starting from the fully closed flap position. By doing this, even the smallest flap-openings can be maintained accurately and reached repeatedly, yielding true proportional control. It is clear that this mode of working offers advantages over traditional methods that utilize open-loop absolute positioning based on counting steps. Because to be sure that the end-stop is reached in a referencing run, these methods require driving the stepper motor multiple steps beyond the estimated end-stop position. This results in a blocked motor with associated acoustic noise and mechanical as well as magnetic wear-out. Now a device that detects the end-stop within one full-step will avoid the noise and vibration during the stall condition. Stall detection within a single full-step also allows the rotor and stator-magnetic fields to remain synchronized. This avoids any risk of magnetic wear-out caused by demagnetization of the rotor due to AC magnetic fields from the stator, and will help to maintain a stable actuator torque over life-time.

Actuator Characteristic	Brush DC	Unipolar Stepper	Bipolar Stepper	Comment
Wear-Out & Durability	-	++	++	no brushes in stepper
Audible Noise	-	+	++	microstepping in bipolar stepper
EMC	-	+	+	commutation sparks in brushed motor
Holding Torque	-	++	++	hold-current in stepper
Sensorless Operation	+	++	++	BDC requires pulse-count if sensorless
Cost of Control Circuit	+	++	-	unipolar requires only 4 low-side switches
Cost of motor	++	-	++	unipolar stepper has 2x Cu vs. bipolar
Number of Wires	2 to 5	5	4	
Stall Detection	++	-	++	recently developed for bipolar stepper
High-speed flap closing	++	-	++	recently developed for bipolar stepper

Table 1: Summary of actuator technologies

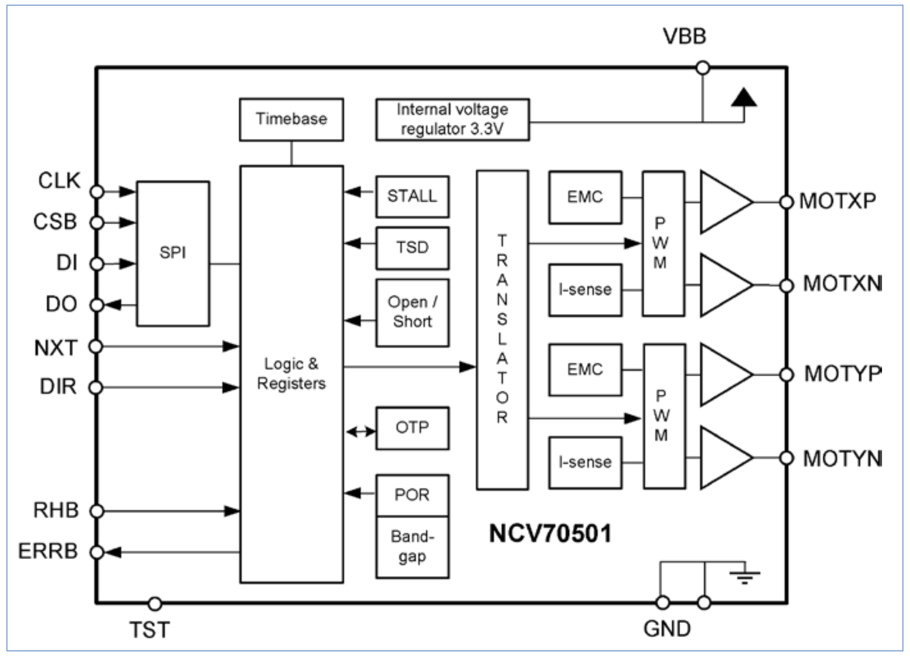

Figure 2: Bipolar stepper motor driver IC (NCV70501) – Block diagram

Speed-critical positioning is important in situations in which a flap needs to be closed as fast as possible: e.g. closing of the recirculation flap when an exterior sensor detects the presence of polluted outside air. The back-emf signal makes speed critical operation possible for stepper motors by means of dedicated adaptive-speed motor drive algorithms. This allows stepper motors to challenge one of the main advantages of brush DC motor actuators, notably the ability to rotate as quickly as the supply voltage and load allows. The stepper motor is operated at the fastest speed possible, adapting speed automatically to the actuator and flap characteristics (e.g. load). During this adaptive-speed operation, sensorless stall detection is operational, guaranteeing error-free positioning. These algorithms allow speeds up to 1000 full steps per second.

Flap Actuator Technologies Summary

Table 1 summarizes the "fit for use" of the flap actuator technologies discussed. Both brush DC and unipolar stepper motors offer their advantages but also show weak points. The new bipolar stepper motor technology seems to offer the best of both worlds and is compatible with all reviewed requirements.

It is up to the Tier-1 HVAC system manufacturers to assign the correct weighting to all these functions. Observation: the system level cost is comparable for the three actuator types, however if only the purchasing cost of the motor driver itself is taken into account, then the car manufacturer might end-up with a sub-optimized solution.

New Recirculation Flap Driver IC

Integrated circuits that drive bipolar stepper motors including the technologies described above are now available. A typical block diagram of such an IC is shown in Figure 2. This IC is placed inside the ECU and two full H-bridges drive the two phases of the bipolar stepper motor. The ECU's microcontroller communicates with the IC via an SPI interface and a set of dedicated signals.

A current translator table, embedded in the driver applies the correct current to the windings. The microcontroller needs to set only once the SPI registers that define the winding current peak value, micro-step mode and default direction of movement. After this, the micro can step through the translator table by applying only "next" signals to the IC (see NXT pin in Figure 2). The motor driver then takes full responsibility and generates the requested current waveforms for full-step, half-step or sinusoidal micro-step motions. The speed of applying the "next" pulses defines the speed of the motor movement.

A simple but highly effective stall detection algorithm is implemented and can be activated by means of the SPI bus. The chip also supports an adaptive speed control function for closing the recirculation flap at maximum speed. Also proper diagnostic functions are implemented to detect all relevant error conditions and to prevent system and IC damage. The IC has an interrupt output pin to warn the microcontroller when an error occurs (see ERRB in Figure 2).

Conclusion

Automatic air recirculation valves can contribute to fuel economy of cars. Existing flap actuator technologies have been discussed in view of operating requirements of such a recirculation valve. Both brushed DC motor actuators and unipolar stepper motor actuators show incompatibilities with some of the technical requirements. A bipolar stepper motor valve in combination with a novel driver offers the best possible technical solution to meet the high-quality operation requirements of the air recirculation valves of the future.

www.onsemi.com

Shining Bright

New approach for driving high-power LED lighting applications

In many high-power lighting applications such as street lights, high-bay stadium lighting and others, the trend is moving towards solid state lighting that uses LEDs as the lighting source. The reason for this adoption is the clear value proposition of higher energy efficiency and less frequent maintenance, both factors justifying the transformation.

By James Aliberti, Product Marketing Engineer, Power Supply Controls, Texas Instruments

In many high-power lighting applications such as street lights, high-bay stadium lighting and others, the trend is moving towards solid state lighting that uses LEDs as the lighting source. The reason for this adoption is the clear value proposition of higher energy efficiency and less frequent maintenance, both factors justifying the transformation.

In these types of high-power lighting applications, a number of different approaches are being considered to drive theses lamps. In this article, we will look at a new topology boasting higher efficiency and lower system cost for driving multiple LED strings.

To adequately measure the merits of this topology, we must first look at the various methods being considered, or that have worked well for lower power LED applications.

One simple method is to use a power supply that converts mains voltage to a DC output voltage such as 12 or 24 volts. Then run parallel LED strings from it and using resistors in each string to regulate current. This is a low-cost approach. However, with today's high-brightness LEDs that can draw currents in excess of 350mA, this approach is very dissipative. It has low efficiency and produces poor current regulation that can cause noticeably different light output from string to string.

To improve on this approach linear regulators replace the resistors, improving the uniformity of the light output of all the strings. But this is the only benefit as there is no noticeable improvement in efficiency or power dissipation. Reducing power dissipation is important to maximize LED life. In these two approaches, using either resistors or linear regulators act as localized heat sources, significantly reducing LED life.

Another method that is also fairly simple is to make a long single series string, using a single power supply that produces a high-voltage DC constant current source. The high-voltage operation in this approach puts it above safety extra-low-voltage (SELV) levels of 60VDC or 42V RMS. It ties the lighting fixture or enclosure to the safety agency approval process and significantly reduces flexibility to apply the same electrical design to other applications.

Another consideration with the single string approach is reliability. If just one LED opens, you loose the light output of the entire fixture. There are measures such as adding many crowbars or devices to clamp each open, but this adds cost and complexity to the light fixture.

The most common method in high-power LED lighting applications is to use multiple string architecture with switching regulators for current regulation. Here a single main power supply converts the AC mains to a single DC bus voltage, usually within the SELV levels. This bus then supplies the parallel LED strings where each string has either a buck (most common) or boost converter. For simplicity sake, we will confine our analysis to the buck, as the boost from a cost and component count is very similar.

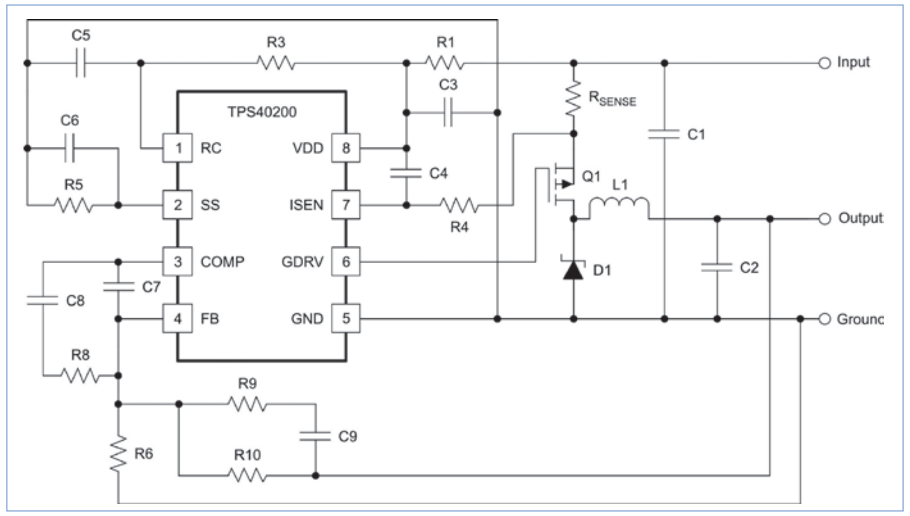

Figure 1: Simple buck regulator

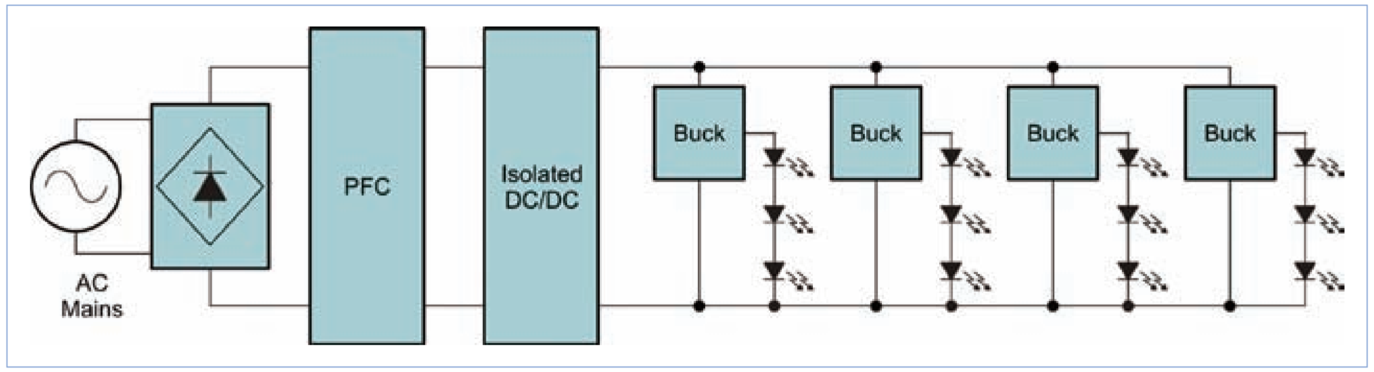

Figure 2: Typical high-power LED lighting system using buck regulators

For example, Figure 1 shows the low-cost simple buck regulator circuit. It consists of a PWM controller, inductor, MOSFET, diode and a handful of resistors and capacitors. If higher efficiency is required, you can replace the diode with a MOSFET and use a PWM controller that enables synchronous buck operation.

Figure 2 shows the various subsystem blocks for a high-power, multiple string lighting application with buck regulators for current regulation.

The AC mains input is rectified and fed to a power factor correction (PFC) boost circuit where the PFC produces a high voltage of 400V, which provides the input to a down stream isolated DC/DC converter. The DC/DC converter output is then used to produce a low-voltage bus, typically 12V or 24V range, providing power to the buck regulated LED strings.

This approach has fairly high efficiency and is a good choice for minimal LED strings. However, for the higher power applications with four or more strings, the component count and cost can really add up. For electronic component manufacturers and the supply chain, this may be an appealing sell. However, for lighting manufacturers and their customers, the high cost can be detrimental to wide adoption. What is needed for solid state lighting's long term viability are low-cost drive circuits that can enable the market to take root and grow unimpeded.

Figure 3 shows a series input, multiple parallel LED (SIMPLE) drive. It is a cost-effective approach for driving multiple LED strings. Excluding the PFC, it is a two-stage approach, comprising an inverted constant current buck regulator and a downstream DC/DC transformer circuit. It is highly efficient, has superior string current regulation and most importantly, a lower cost approach. It also can have inherent redundancy with a single passive acting silicon-controlled rectifier (SCR) crowbar added for each string. If an LED or string opens, it will not take down the remaining strings.

Before we go into the operation, let's look at some of the things that immediately stand out when using the SIMPLE drive multi-transformer approach. First, notice that this is an electrically isolated design where secondary side output voltages can be designed to stay within SELV levels. When the output voltage stays within SELV levels, it eliminates the requirement to have the lighting fixture combined with the power supply, and interconnects to have safety agency approvals. Having the output within these levels adds inherent flexibility, allowing many varieties of fixtures addressing many other lighting applications. The power supply still requires safety approvals, just like all the off-line solutions discussed in this paper, but not the light fixture.

dditionally, the isolated design can be significantly better from a thermal management perspective as there are no restrictions for LED proximity or contact to metal enclosures. Another feature that stands out is that it does not require feedback from the output side. This eliminates an opto or some other safety rated isolated feedback device. Finally, look at the simplicity of the sec-

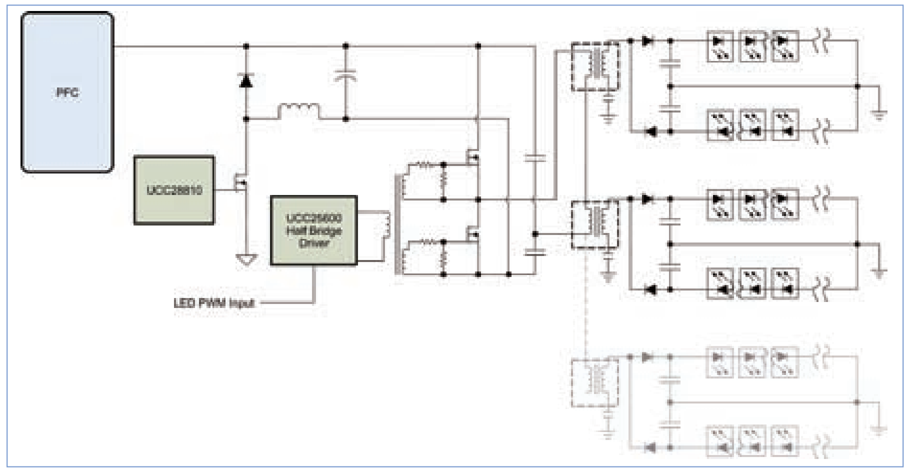

Figure 3: SIMPLE drive multi-transformer

ondary side. It has only a few passive components, and no bias supply, active components or control of any kind.

When it comes to operation, the SIMPLE drive has superior string current matching of better than one percent. It has resonant operation for high efficiency and becomes more cost effective as the number of strings increases.

General Description

The output of the PFC circuit is the input of the inverted buck circuit. The inverted buck is configured to produce a constant current output. It is this current where the systems closed loop is around. The current output it produces is fed downstream to the DC/DC transformer circuit, which consists of a half-bridge controller, two MOSFETs, capacitors C1 and C2, and the transformers. This current is then circulated through the half-bridge MOSFET switches to the primary sides of the series transformers. Capacitors C1 and C2 serve a number of functions. They are used to set up a voltage divider for the half-bridge, are elements of the resonant circuit, and are DC-blocking capacitors, which help to prevent transformer saturation.

The resonant operation allows the MOSFET switches to switch with zero voltage switching (ZVS). This reduces switching losses and forces the output diodes to zero current switch (ZCS), both adding to maximize efficiency.

The DC current, now transformed to AC current, resonates back and forth through the primary side of all the series transformers. The number of transformer primaries that can be put in series is quite flexible as the winding ratios can be selected to support many transformers or LED strings. What needs to be considered for calculating turns ratios is the number of strings, as this dictates the number of transformers and the forward voltage of each string.

Design Considerations

To achieve the highest possible efficiency in power conversion, the goal is to process the least amount of power as possible. To do this, we need to work as close to the input voltage as possible. Since most high-power lighting applications favor the use of active PFC, for simplification purposes we will just consider it as a functional block and assign some typical values to its output

Since most active PFC circuits operate as a voltage boost, a PFC output voltage must be set higher than the peak of the highest AC line voltage. With a universal input range of 85 – 265VAC, this comes to about 375V. Adding some headroom for margin and tolerances, 400V has become a typical set point. To make sure that downstream buck has plenty of headroom from the output variations of the PFC, add a little more margin for ripple of about 40V. This makes our minimum input operating point for the inverted buck at about 360V.

To assure that the buck output has some compliance voltage for it to work properly, give it some headroom as well and limit its output range to 280V.

Now that we know our boundaries, let's look at a design example on how to calculate the value of the constant current from the buck and the transformers' turns ratio.

In this example we use two transformers to drive four LED strings with 1A current. Each string has ten high-power LEDs.

Assumptions: LED forward voltage Vf = 3.5V with a string voltage = 35V

Since we set the output operating point of the DC buck at 280V, it now acts as the input to the DC/DC transformer circuit. This means that the voltage applied to the series primaries will be half that voltage from the capacitor voltage divider made up of C1 and C2, giving us 140V across the series primary arrangement.

Calculating the turns ratio now becomes fairly easy as Equation 1 indicates:

Primary Voltage (VP) of each Transformer = Bridge Voltage / Num Transformers = 140V/2 = 70V

$$\frac{N_P}{N_S} = \frac{V_S}{V_P} = \frac{35V}{70V} = \frac{1}{2} =$$

A turns ratio of 2:1 (Equation 1)

Where:

N_P = Number of turns on the primary

N_S = Number of turns on the secondary

V_S = Secondary side or LED string voltage

V_P = Voltage across each primary winding

To calculate the inverted bucks' current output set point, where each transformer drives two LED strings, it first must be recognized that only one string in each transformer is conducting in alternate half cycles. This means that the current that must be delivered to the conducting string to sustain LED conduction during the dormant period must be twice the LED current. In this case where 1A is the desired LED current, the current delivered to the LED and filter capacitor each half cycle is 2A.

To calculate the buck regulator, set current point (ISet) is in Equation 2:

$$I_{Set} = I_{LEDs} \bullet \frac{N_S}{N_P} = (1\ \text{A})\frac{1}{2} = 0.5\text{A}$$

(Equation 2)

Conclusion

As can be seen, it is a very simple exercise to determine the transformer requirements, and makes the SIMPLE drive a very flexible solution to address a number of different lighting applications. If you intend to make SIMPLE drive as part of a modular approach strategy to your many LED lighting applications; you need to consider the upstream power stages such as power handling components in the half-bridge, inverted buck, and PFC as they must be sized to handle the highest power level you expect the drive to address.

For more information about the SIMPLE drive multi-transformer, including reference designs, see the product folder for UCC28810: www.ti.com/ucc28810-ca, or evaluation module: www.ti.com/ucc28810evm003-ca.

www.ti.com

Fairchild Semiconductor

FAN7621 – Integrated PFM Controller

The FAN7621 is an integrated PFM controller for half-bridge resonant applications up to 600W such as video game consoles, telecom power supplies, desktop PCs, PDP and LCD TVs. This all-in-one solution simplifies design and improves efficiency, eliminates external components, reduces switching losses in MOSFETs and rectifiers, and boosts noise immunity to guarantee stable operation. Compared to conventional hard-switching converter topologies, the FAN7621 improves efficiency for applications such as PDP-TVs by 97%. Visit the Fairchild Semiconductor website to learn more about the FAN7621,

www.fairchildsemi.com/pf/FA/FAN7621.html

International Rectifier

IR's new web-based tool enables the rapid selection and simulation of selected SupIRBuck products. Based on a designer's given input and output parameters, the SupIRBuck online tool selects suitable devices for a given application

www.irf.com

Infineon

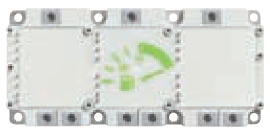

HybridPACK™ 2 - Compact Power for Your Electric Drive Train.

Based on the long time experience in the development of IGBT power modules and intense research efforts of new material combinations and assembly technologies, Infineon has developed – dedicated for automotive applications – this HybridPACK™ 2 power module belonging to the HybridPACK™ family. With its pin fin base plate for direct water cooling Infineon HybridPACK™ 2 is designed to fulfill the requirements of your electric drive train application with power ratings of up to 80kW.

www.infineon.com/cms/en/product/channel.html?channel=db3a3043136fc1dd011370e812b7043a

LEM

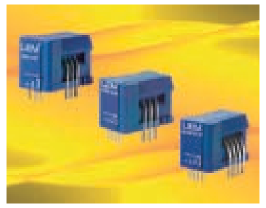

This year, LEM will be highlighting a range of products, including the CAS, CASR and CKSR family of current transducers. They are suitable for industrial applications such as variable speed drives, UPS, SMPS, air conditioning, home appliances, solar inverters and also precision systems such as servo drives for wafer production and high-accuracy robots.

LEM is a leading manufacturer of current and voltage transducers used in a broad range of industrial applications, including variable speed drives for motors and power supplies, AC/DC converters, UPS systems for computers as well as in new innovative energy applications, such as micro-turbines, wind and solar power generation.

For further information please go to

www.lem.com

ITW Paktron

Non-Polarized Polymer Film Capacitors (CS Series) Designed for Mission Critical Applications

ITW Paktron's Multilayer Polymer (MLP) Film Capacitors (Type CS Series) feature ultra-low ESR and high ripple current capability and are designed for high frequency filtering and EMI/RFI suppression in power conversion applications. Provides mechanical and electrical stability, compared to multilayer ceramic capacitors. Features "non-shorting" operation and does not crack like large ceramic chip capacitors under temperature extremes or high vibration. There are no DC or AC voltage coefficient issues with polymer film capacitors.

Capacitance values range from 0.33µF to 20µF and voltage ratings are 50 to 500 VDC. Lead time is stock or four to six weeks.

www.paktron.com

Cool Running Autos

Cooling of IGBT based power modules for Hybrid Electric and Electric Vehicles

It has been forecast that by 2020 there will be upwards of 10 million passenger and light truck vehicles sold annually that are powered entirely or in part by electric motors. Starting with the leadership of Toyota's first Hybrid car launched in 1997, significant progress in various power train electrification designs have been made by every major OEM, especially during the last five years.

By Thomas Sleasman and Birol Sonuparlak, Thermal Management Solutions, Rogers Corporation, Chandler, Arizona, U.S.

Today's Hybrid Electric Vehicle Power Module Market

Hybrid drive systems use a combination of an internal combustion engine (ICE) and one or more electrical motors (EM). Variations in hybrid drive systems depend on how the EM and ICE of a power train connect, and also when and at which power level each propulsion system contributes to powering the vehicle.

There are two types of HEV drive systems, series or parallel. The parallel system is currently used by almost all the major OEMs. Parallel hybrid systems can be further categorized as assist, mild and full hybrid. The Toyota Prius and the Ford Escape are examples of full hybrids, as they can run on just the ICE, the EM or a combination of both. Mild hybrids on the other hand do not run on EM only. The EM provides additional power as required while the ICE still provides the primary power for the power train. Honda's Integrated Motor Assist (IMA) is such a mild hybrid. A third hybrid drive system is the plug-in hybrid (PHEV). These should be increasingly popular in the future. PHEV allows the driver to choose the mode of operation. The driver can choose the EM mode of operation for short distance commuting or the independent ICE mode of operation for long distance driving. The PHEV's larger battery can be charged using standard voltages from a typical power grid system.

Electric vehicles (EVs) are also receiving renewed attention. The electric motor (EM) is the only source of propulsion in EVs. Prior to 2003, most of the major OEM's, such as Chrysler, Ford, GM, Honda, Nissan and Toyota, produced a limited number of EVs. More recently, a Renault-Nissan alliance has started developing a complete range of 100% electric power trains with power ratings of 50kW to100kW. Renault has already announced the final production design of two electrical vehicles, Fluence ZE and Kangoo ZE. The Fluence production plant will start manufacturing this sedan in the first half of 2011 at the Bursa OYAK-Renault plant in Turkey. Renault forecasts 100,000 vehicle sales over five years starting in 2011. The Fluence will also be the first EV to test the Better Place battery swap concept in Israel.

HEV/EV Power Module Solutions

The efficient dissipation of heat generated by Insulated Gate Bipolar Transistor (IGBT) based power modules used to control these electric drive designs is critical to system quality and reliability. Design concepts such as integrating inverter, DC-DC converter and electronic control unit, along with reducing the number of IGBT power chips, are helping design engineers to lower the size and weight of the power train and significantly reduce the power train cost. Reducing the size and populating more components in a confined space increases the challenges of thermal management. Well engineered thermal management is required to cool electronics and maintain electrical performance within a given envelope of HEV/EV operation, and efficient thermal management provides long term reliability by minimizing thermally induced stresses.

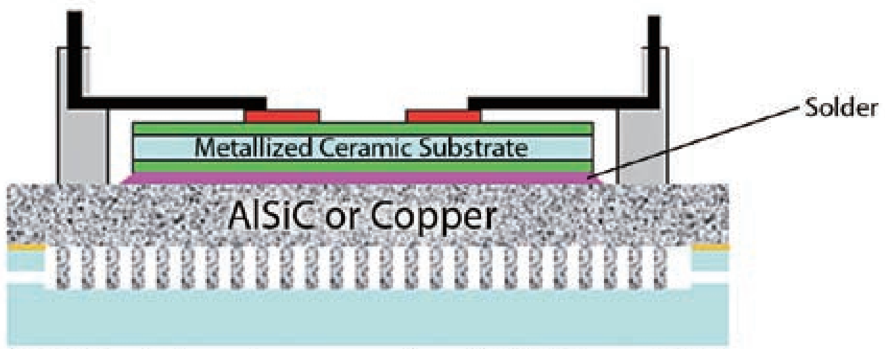

FIGURE 1 — Schematic representation of HEV/EV Power Module

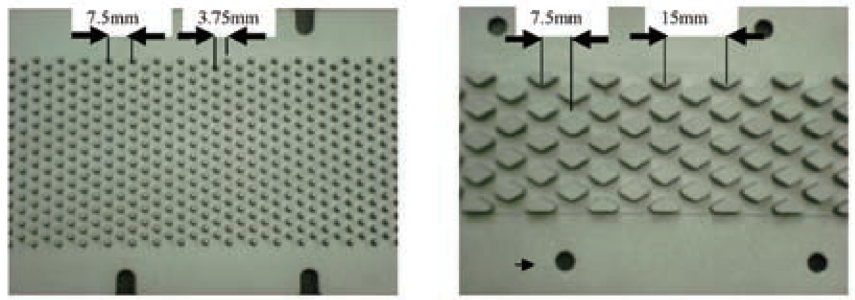

Figure 2. Examples of AlSiC baseplate pin designs

The need to be light weight, smaller in size, more efficient in energy use, less costly and able to meet stringent automobile and transportation standards is being addressed today by manufacturers of direct liquid cooled Pin Fin IGBT base plates produced in copper and aluminum silicon carbide reinforced metal matrix composites. These products and their application to power electronics are mature, well known and, as we explore in this article, well positioned to realize the design goals of current and future Hybrid and Electric vehicles.

Today, most HEV/EV inverter systems use liquid cooled IGBT power modules for thermal management. Although there are still power module designs utilizing air cooled power modules in design and production, we believe that future IGBT power modules for HEV/EV applications will continue to use more direct liquid cooled IGBT modules and move heat away from these modules more efficiently. A schematic representation of IGBT power module with pin fin heat sink is illustrated in Figure 1.

Integrated Pin Fin, direct liquid cooling base plates eliminate thermal grease interfaces between the IGBT module and the heat sink. This is a performance advantage that is realized in HEV/EV IGBT power modules beyond the standard base plate technology currently used in power modules for Rail/Traction power IGBT modules. Today, 70 to 80% of standard power modules for HEV/EV use base plates. There are also power modules on the market that do not use base plate solutions. These solutions also eliminate the solder joint between the DBC and base plate, and are present in such products as the SKAI IGBT System and Danfoss Shower Power® cooler system.

Today, pin fin heat sink material selection is made generally between copper and AlSiC materials. AlSiC pin fin designs used in HEV/EV IGBT power module applications are illustrated in Figure 2. While the majority of HEV/EV IGBT power modules in design today use pin fin base plates made from AlSiC MMC or copper, there are developmental designs that use 100% aluminum pin fin base plates. In these developmental designs, the thermal resistance of the IGBT module will be considerably reduced by eliminating the solder joint between the ceramic substrate and the pin fin heat sink. The long term reliability and the cost advantages of these developmental designs still need to be demonstrated.

Base Plate Selection Considerations

Selection of the base plate material is usually made based on the reliability requirements in the application as well as the choice of ceramic substrate materials. The properties of pin fin base plates and ceramic substrates used in IGBT power modules are listed in Table 1.

Ceramic substrate choices are silicon nitride, aluminum nitride and aluminum oxide. Considering that many HEV/EV applications require 15 to 20 years of useful life, AlSiC pin fin heat sinks joined to metalized aluminum nitride or silicon nitride substrates have become the preferred choice. This AlSiC heat sink/ceramic substrate combination not only provides excellent thermo-mechanical stability due to the close CTE match between the AlSiC base plate and the ceramic substrates and maximizes long-term reliability, it also provides proper cooling of the IGBT chips.

A close CTE match between the ceramic substrate and AlSiC is a fundamental advantage in preventing any failure during thermal cycling. When thermal cycling power modules with copper base plates, almost all the interfaces, including the Si chip/DBC interface, are in danger of delamination, fatigue and crack propagation. These failure modes are accelerated when the ceramic is AlN due to this material's lower CTE. An alumina (Al_2O_3) substrate is generally preferred to AlN to reduce the probability of failure of a power module when a copper base plate is used. Due solely to the degree of CTE matching of the system, the heat dissipation performance of a power module with AlSiC base plates will remain consistent even after thousands of thermal cycles, while the thermal performance of power modules with copper bases will gradually decrease after each thermal cycle.

This restriction in selection of ceramic substrates translates into another potential shortcoming of power modules utilizing copper base plate technology. When properties are examined, the primary advantage of copper to AlSiC is copper's high thermal conductivity. However, when copper base plate is used with aluminum oxide substrates, heat dissipation through the base plate is reduced due to the presence of aluminum oxide as a thermal barrier between the IGBT chip and the copper base plate.

In contrast, AlSiC base plate power modules that use AlN as the ceramic substrate do not exhibit this problem. The high thermal conductivity of AlN and the inherent CTE compatibility between AlN and AlSiC, contribute to a high reliability design. When Si3N4 is selected as the substrate material instead of AlN, the thickness of the ceramic substrate can be reduced and the thickness of the copper layers can be increased. This is because Si3N4 is a much stronger material than AIN and Alumina. AlSiC/ Si3N4 will still provide the better solution than copper/Si3N4 solution for the same reasons described above.

Yet another design advantage for AlSiC base plate technology is the superior stiffness of AlSiC when compared to copper and aluminum. AlSiC materials' mechanical properties allow designers to reduce base plate thickness, allowing for reductions in Power Module space requirements. AlSiC plates remain flatter after ceramic soldering processing steps. Copper base plates change flatness more than AlSiC during soldering processes and also tend to relax over time as stresses are gradually released. It can take weeks for the stresses to completely stabilize after soldering. In contrast, the flatness in an AlSiC base plate becomes stable within a day or so. This predictability makes manufacturing of IGBT modules simpler and allows for better control in the assembly process.

	TC (W/mK)	CTE (ppm/K)	Density (g/cc)	Thickness (mm)
AlN Substrate	170	4.2	3.26	0.64
Si_3N_4 Substrate	70 - 90	3.4	3.2	0.32
Al_2O_3 Substrate	24	7.1		0.25 – 0.38
AlSiC Pin Fin Heat Sink	170 - 230	5-14	2.8 – 3.08	3
Copper Pin Fin Heat Sink	390	16.9	8.9	3

Table 1: Baseplate and ceramic materials used in IGBT power modules

Price Considerations

Although the performance advantages of AlSiC in HEV/EV applications are clearly understood, there are still misconceptions in terms of pin fin heat sink unit prices when AlSiC and copper are compared. Based on the flat or partially bowed IGBT base plate comparison between AlSiC and copper in traction applications, engineers can be lead to believe that AlSiC pin fin heat sinks would be 3 to 4 times more expensive than copper pin fin heat sinks. In reality, manufacturing processes allow AlSiC pin fin heat sink and copper fin heat sinks to have costs that are very comparable. The manufacturing process costs of pin fin copper base plate are much higher than the stamped copper used in traction applications.

In conclusion, the engineered properties of SiC reinforced aluminum composites and net shape capabilities to produce pin fin AlSiC composite parts have now been recognized by many TIER 1 suppliers for HEV/EV IGBT power module applications. AlSiC price concerns are being eliminated when companies think through designs that utilize the broad advantages of AlSiC pin fin heat sinks over traditional copper or aluminum materials.

www.rogerscorp.com

Rugged Vehicle Applications Drive Search for Seasoned Engineers in Heavy Equipment Industry

By David G. Morrison, Editor, How2Power.com

Engineers who design power converters for automotive applications must grapple with extreme environmental conditions including very wide temperature ranges and severe shock and vibration. At the same time, they must ensure that their converters operate with high reliability. These challenges only get worse when the end application isn't a car or light truck intended to travel paved streets and highways, but off-road vehicles such as construction or farming equipment (a.k.a heavy equipment). These are the types of environmental conditions that relatively few engineers will learn about in their professional work. And almost none will encounter these conditions as students studying electrical engineering.

So, it should come as no surprise that international original equipment manufacturers (OEMs) such as John Deere, which build heavy equipment, specifically seek out power electronics engineers with experience in the same or a closely aligned industry. That experience is in addition to educational requirements for an advanced EE degree with an emphasis on power electronics. Plus, there are additional qualifications such

as a background in high-power design, and in electric/hybrid electric vehicle design. These types of experience, though not necessarily required, do make job candidates more attractive to OEMs in the heavy equipment industry.

At present, finding engineers with all of these qualifications can be a challenge, as Chad Haedt, a product engineering recruiter for John Deere's North American operations, explains.

Many Candidates, But Not Enough Experience

There are a few reasons why qualified engineering candidates are not available to OEMs who build heavy equipment.

"Right now [finding qualified candidates] is a difficult task. The reasons are strong growth across a number of industry sectors (not just ours) related to power electronics. The majority of candidates we see are more-recent graduates or candidates with advanced degrees that don't have the industry experience," says Haedt. He notes that his company seeks out those who have "have experience in designing ruggedized power electronics systems for harsh environments and vehicle applications in heavy equipment markets."

Haedt says that his company receives many applications for power electronics engineering positions. In fact, there are more applicants for these positions than for those involving other types of electronic hardware design. However, "we don't get nearly as many qualified applicants" for the power electronics design jobs as for positions in standard hardware design.

Curiously, the company does hire many electrical engineers right out of school, just not for the power electronics design positions. Haedt explains that while power electronics is a growing area within John Deere's business, it's still a relatively small segment within the organization—one that employs more than 50,000 people globally. As a consequence, the company seeks out only experienced power electronics engineers—at least for now. However, for some of these positions, candidates can qualify with as little as three years' time in industry (or even less for someone with an advanced degree. (See the table accompanying the online version of this article for example job descriptions.)

Competition for such experienced candidates comes from within the heavy equipment industry, from its suppliers, and from the automotive industry, says Haedt. And not just from established companies, says Haedt, but also from startup companies funded by research or venture capital.

Competition and scarcity of qualified candidates works in the favor of those who do make the cut. Haedt notes that at John Deere engineers hired for power electronics design jobs are likely to be compensated at a higher level than electrical engineers working in other areas. Although Haedt declines to say how much more these engineers may receive, he indicates that there is not "a drastic difference" in pay between power electronics and other EE positions.

The Right Industry Experience Is Key

Since industry experience is so important at heavy equipment companies such as John Deere, it's worth noting what type of experience these companies value.

"Automotive OEM candidates as well as candidates from tier one automotive suppliers are very good," says Haedt. "We consistently look for those candidates."

According to Haedt, that's because engineers working in the automotive industry use design processes and quality standards that are similar to those used in the heavy equipment industry.

"In automotive as well as off-road, well defined requirements, design processes, design gate reviews, very thorough design analysis and qualification testing are key," says Haedt. "The difference is doing that in our environment because you're talking about dirt, soil and wind, off-road terrain, all different types of temperatures. You get that in automotive, but with our applications, they're much more harsh."

These more-challenging environmental conditions lead to more vigorous testing in the heavy equipment industry. Nevertheless those differences in testing (from what's applied in the automotive industry) can be learned on the job.

Power electronics engineers who've worked in the mil/aerospace industry are also considered good job candidates—just as they are by companies in the automotive business. As in the heavy equipment industry, designers who work in the mil/aerospace industry deal with harsh environments and demands for high reliability. According to Haedt, the level of design analysis and qualification testing required in mil/aerospace applications is considered good preparation for what's required in the heavy equipment industry.

Candidates who have these types of industry experience can distinguish themselves further if they have system-level knowledge of hybrid or electric vehicles. Haedt comments that even though his company doesn't typically require such knowledge, it's considered "extremely valuable."

"Right now, the demand for experienced engineers in that area [hybrid or electric vehicles] is higher than the resource pool, but we think eventually the gap could be reduced as there are a lot of students interested in getting into these areas," says Haedt.

Education Is Still Fundamental

Despite all their interest in a candidate's previous employment, OEMs still value university training. Haedt says his company is looking for candidates with a master's degree or PhD with emphasis in power electronics.

It also doesn't hurt to have a degree from one of the established power electronics programs. Although John Deere doesn't recruit candidates directly from such schools, it considers them highly attractive candidates once they've acquired some industry experience.

In some cases, an applicant's academic background can help bridge the gap between working in related industries like automotive and working in the heavy equipment business. For example, the power levels encountered by designers in the latter industry are likely to be higher than those seen in automotive. However, if as students, these job applicants have done research or project work in higher power areas, "that's a good fit for us" says Haedt.

Not every candidate must have the background of designing for higher-power applications. Nor must they be a perfect match in every regard. For example, if a candidate has credentials that are close to what John Deere is looking for, but needs more work in high-power applications, says Haedt, "we have people that can train and develop newer engineers."

For examples of job opportunities for power electronics engineers in the heavy equipment industry, see the table listing sample positions in the online version of this article. For some some perspective on the similarities between this industry and automotive, see "Hybrid Vehicles Drive New Demands for Power Electronics Expertise" in the January issue of How2Power Today.

About the Author

David G. Morrison is the editor of How2Power.com, a site designed to speed your search for power supply design information. Morrison is also the editor of How2Power Today, a free monthly newsletter presenting design techniques for power conversion, new power components, and career opportunities in power electronics. Subscribe to the newsletter by visiting

www.how2power.com/newsletters/

Auto Gets Cleaner

Reported by Cliff Keys, Editor-in-Chief, PSDE

With automotive systems consuming more and more semiconductor devices for their control, safety and comfort specifications, the main focus has been to add more of these goodies to pull in the customers. On the other side of power engineering for the automotive sector, is the urgent development of affordable hybrid electric and battery electric vehicles.

All this is great news for the environment and for power engineering in general, but for the foreseeable future we will continue to see (and breathe) conventionally powered vehicles. Here too, engineering is hard at work for our benefit.

Simulating exhaust systems

The limits for nitrates in diesel engine emissions defined by international standards such as EURO 6 (in the European Union) and EPA 2010 TIER IV (from the USA's Environmental Protection Agency) are becoming increasingly strict. Compliance with these tougher limits is not possible without electronically controlled catalytic converters. Selective catalytic reduction (SCR) systems that use urea injection (with AdBlue) are an especially effective solution. Simulating the control algorithms plays a vital role in the development of these systems.

The ASM Diesel Exhaust Model, one of the Automotive Simulation Models (ASMs) from the leading producer of engineering tools, dSPACE, provides a complete virtual diesel exhaust aftertreatment system. In addition to the submodel for urea injection (the SCR system), it includes further submodels for a diesel oxidation catalyst (DOC) and a diesel particle filter (DPF). The simulation model can be used throughout the development process, from controller design in Simulink® to ECU testing on a dSPACE simulator.

A special feature of the model is that users have complete access to all its Simulink blocks. They profit from being able to view the modeled functions and adapt them to specific requirements themselves. The exhaust model's individual components (DOC, DPF, SCR) can be combined in different ways and optimally configured for the aftertreatment system under test.

The model can be used to represent the essential physical and chemical processes in modern aftertreatment systems: urea decomposition for catalytic reduction, fuel post-injections for catalytic oxidation, soot particle filtering and DPF regeneration. It contains AdBlue dosing systems with and without air supply and simulates temperature, pressure and lambda sensors, providing everything necessary for efficiently developing and testing controllers for modern diesel exhaust aftertreatment systems.

Global PV market to double in 2010

The global PV market will almost double in 2010 to reach a massive 14.6GW, nearly three times size of the market back in 2008. IMS Research has analyzed PV demand in more than 40 countries globally. In addition, the forecast is based on a survey of inverter suppliers which analyzed the inverter industry's production for 2010.

www.powersystemsdesign.com/greenpage.htm

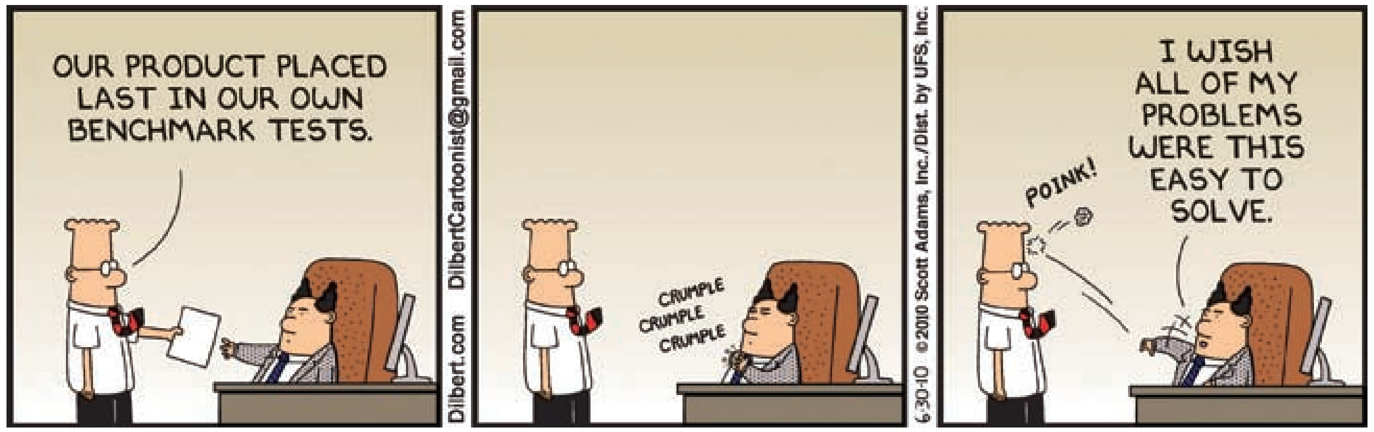

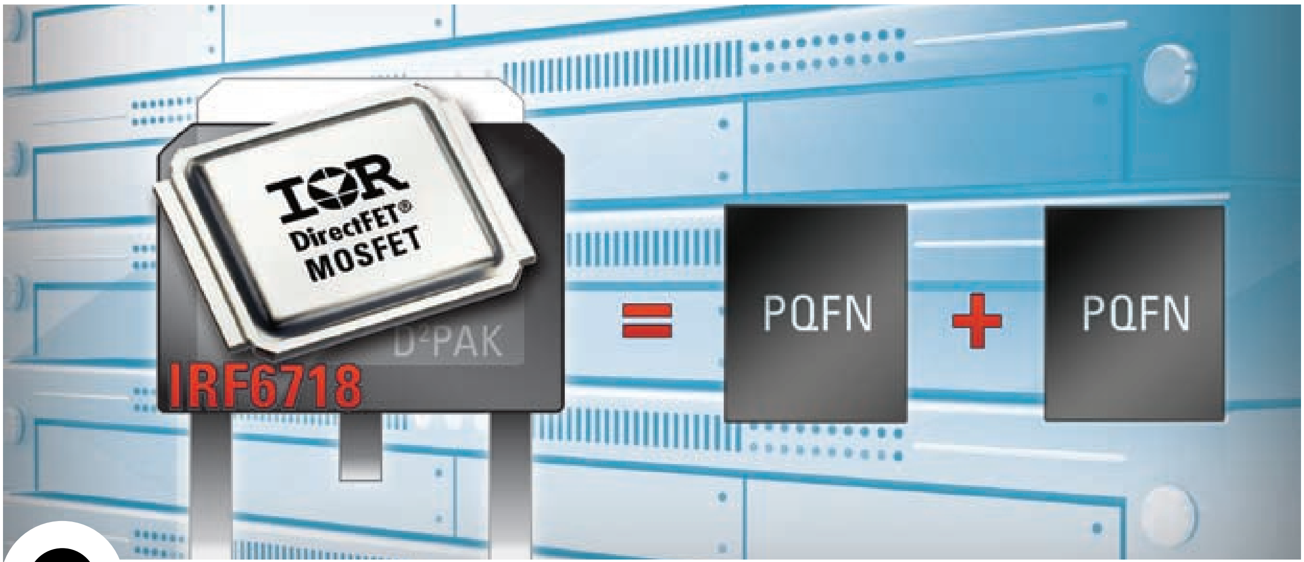

IR's IRF6718 Large Can DirectFET® MOSFET Delivers Industry's Lowest $R_{DS(ON)}$*

Optimized for Active ORing and Hot Swap Applications

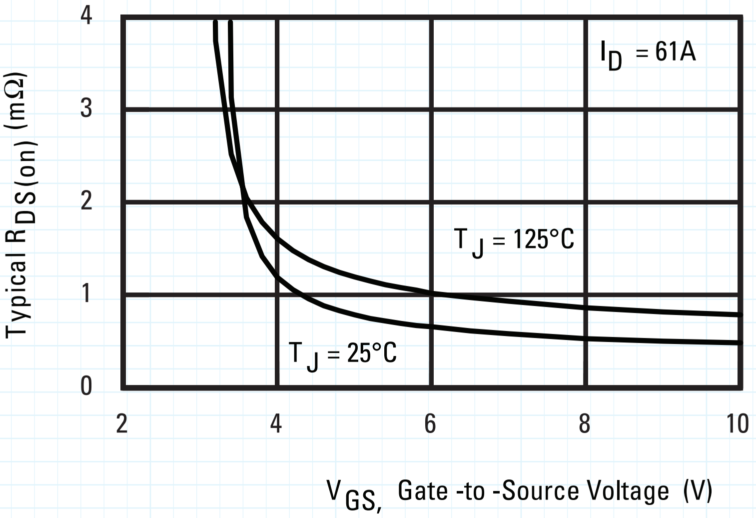

The IRF6718L2 features IR's latest generation silicon technology in a new large can DirectFET® package delivering extremely low $R_{DS(on)}$ of only 0.5mOhm (typical) at 10V VGS in a 60% smaller footprint and 85% lower profile than a D²PAK. The IRF6718L2 significantly reduces conduction losses associated with the pass element in ORing or hot swap applications to dramatically improve the efficiency of the entire system.

FEATURES

- Industry Lowest $R_{DS(on)}$ for Reduced Conduction Losses
- Superior electrical and thermal performance in smaller footprint than D²Pak
- Dual-sided Cooling Compatible
- Reduces component count and board space compared to competing solutions
- Compatible with existing Surface Mount Techniques
- RoHS Compliant Containing no Lead or Bromide

Part Number	Package Size (mm x mm)	$R_{DS(on)}$ @10V typ. (mΩ)	I_D @ TA = 25°C (A)
IRF6718	7.1 x 9.1	0.5	270
Competitor 1	10.7 x 15.9	0.7	180
Competitor 2	5.1 x 6.1	0.95	60
Competitor 3	5.1 x 6.1	1.5	65

* Based on data compiled September 2009

for more information call +49.6102.884.311 or visit us at www.irf.com

DirectFET® is a registered trademark of International Rectifier Corp.